Check for updates

DATA NOTE

REVISED Dissipate and Recentre (D&R) experimental campaign on real scale GFRP composite frame structures: data set

[version 2; peer review: 3 approved, 1 approved with reservations]

José Gonilha[1,2], João Ramôa Correia[2,3], Manuela Buttazzi[4], Francesco Ciani[4], Francisco Javier Molina[5], Simone Peloso[5]

[1]IDMEC, Instituto Superior Técnico, Universidade de Lisboa, Lisbon, Portugal
[2]DECivil, Instituto Superior Técnico, Universidade de Lisboa, Lisbon, Portugal
[3]CERIS, Instituto Superior Técnico, Universidade de Lisboa, Lisbon, Portugal
[4]MM s.r.l. a Socio Unico, Udine, Italy
[5]European Commission Joint Research Centre Ispra, Ispra, Lombardy, Italy

v2 **First published:** 08 Oct 2025, **5**:308
https://doi.org/10.12688/openreseurope.20500.1
Latest published: 14 Jan 2026, **5**:308
https://doi.org/10.12688/openreseurope.20500.2

Abstract

In the scope of the Dissipate&Recentre project, which was granted access to the ELSA Reaction Wall of the Joint Research Centre physical research infrastructure of the European Commission, large scale composite frame structures were tested under lateral loading. The test specimens, comprising pultruded glass fibre reinforced polymer (GFRP) profiles, connected with stainless steel elements, had two longitudinal (test direction) bays, two storeys and a shorter transverse bay. Concrete slabs were provided as flooring system, simulating a quasi-permanent load level – as that used in seismic design. A total of 4 full-scale specimens were tested, two including a bracing system, also comprising pultruded GFRP profiles, and two without bracings. For each configuration, one specimen was tested under monotonic loading and the other under cyclic loading. The aim of this paper is to disseminate the experimental data obtained in these tests. To that end, the experimental campaign is thoroughly described, including all the relevant details of the test specimens, the construction process, the setup and instrumentation, and the test programme. Additionally, a brief description of the test observations is also provided. The test results showed that the structural integrity of these GFRP frames was maintained up to 2% inter-storey drifts, for both braced and unbraced configurations, presenting very limited damage. These results indicate that GFRP frame structures may be designed to withstand significant seismic actions.

Open Peer Review

Approval Status ✓ ? ✓ ✓

	1	2	3	4
version 2 (revision) 14 Jan 2026	✓ view		✓ view	✓ view
version 1 08 Oct 2025	✓ view	? view		

1. **Marco Civera**, Polytechnic of Turin, Turin, Italy
2. **Haitham Al-Thairy**, University of Al-Qadisiyah, Al Diwaniyah, Iraq
3. **Mohammadreza Vafaei**, Universiti Teknologi Malaysia, Johor, Malaysia
4. **Angelo Savio Calabrese**, Politecnico di Milano, Milan, Italy

Any reports and responses or comments on the article can be found at the end of the article.

Keywords
GFRP, Seismic design, Eurocode, Cyclic testing, Large-scale tests

This article is included in the Joint Research Centre gateway.

Corresponding author: José Gonilha (jose.gonilha@tecnico.ulisboa.pt)

Author roles: Gonilha J: Conceptualization, Funding Acquisition, Investigation, Methodology, Project Administration, Validation, Writing – Original Draft Preparation; **Ramôa Correia J**: Conceptualization, Investigation, Methodology, Writing – Review & Editing; **Buttazzi M**: Funding Acquisition, Investigation, Resources, Writing – Original Draft Preparation; **Ciani F**: Funding Acquisition, Resources, Writing – Review & Editing; **Molina FJ**: Data Curation, Methodology, Writing – Review & Editing; **Peloso S**: Data Curation, Methodology, Writing – Original Draft Preparation

Competing interests: The third and fourth authors are employees of M.M. Srl, which is a partner of the project and funded the specimens. M.M. Srl commercializes the pultruded profiles used in the experiments and may commercialize the structural solutions developed.

Grant information: The experimental data used in this research were generated through access to the ELSA Reaction Wall under the framework of access to the Joint Research Centre physical research Infrastructures of the European Commission (Dissipate&Recentre project, Research Infrastructure Access Agreement Nr. 36506-2/2021-1-RD-ELSA-ReactionWall). The first author acknowledges Fundação para a Ciência e a Tecnologia (FCT) for its financial support via the project LAETA Base Funding (DOI: 10.54499/UIDB/50022/2020). He also acknowledges the support of FCT through the financing of his research contract (DOI: 2023.06116.CEECIND/CP2859/CT0001). The second author also acknowledges FCT for its financial support through CERIS (DOI: 10.5449/UIDB/04625/2020).
The funders had no role in study design, data collection and analysis, decision to publish, or preparation of the manuscript.

Copyright: © 2026 Gonilha J *et al*. This is an open access article distributed under the terms of the Creative Commons Attribution License , which permits unrestricted use, distribution, and reproduction in any medium, provided the original work is properly cited.

How to cite this article: Gonilha J, Ramôa Correia J, Buttazzi M *et al.* **Dissipate and Recentre (D&R) experimental campaign on real scale GFRP composite frame structures: data set [version 2; peer review: 3 approved, 1 approved with reservations]** Open Research Europe 2026, **5**:308 https://doi.org/10.12688/openreseurope.20500.2

First published: 08 Oct 2025, **5**:308 https://doi.org/10.12688/openreseurope.20500.1

REVISED **Amendments from Version 1**

Following the reviewers comments we have updated 4 figures Figure 39, Figure 40, Figure 41, and Figure 43, changing the order of the legend. We have also included Grant information which was missing on the previous version.

Any further responses from the reviewers can be found at the end of the article

Introduction

Over the past decades, fibre reinforced polymer (FRP) composites have been increasingly used as structural materials in the construction industry, owing to their high strength, low self-weight, non-corrodibility and reduced maintenance costs[1]. Among FRP composites, pultruded Glass-FRP (GFRP) profiles are an especially attractive solution for new construction and rehabilitation, due to their competitive cost. Moreover, their high durability guarantees long service life and bolted connections enable the design of demountable structures, thus promoting the sustainability of the construction industry and aligning with the priorities of the European Commission (Green Deal and New European Bauhaus) and of the Joint Research Centre (JRC) infrastructure (design and retrofit for resilience, new materials and technologies, and sustainable materials for construction).

On the other hand, pultruded GFRP profiles typically present brittle failure modes, which contrast with current design philosophies that aim at exploiting material (and system) ductility. This has raised well-founded concerns about the application of GFRP profiles in seismic areas, which is aggravated by the lack of comprehensive seismic design guidance. Previous research conducted at IST-ULisboa has addressed this concern, through the development of improved beam-to-column bolted connections[2–6], and the study of two-dimensional[7,8] and three-dimensional[9] pultruded GFRP frames.

This paper presents the data set of the Dissipate and Recentre (D&R) project, which aims at experimentally investigating the sway behaviour of large-scale GFRP frames. The objectives of the project are to assess the behaviour of these structures under lateral loading, assessing and proposing seismic design methods and guidelines. The experimental campaign was performed at the European Laboratory for Structural Assessment (ELSA) of the JRC, and the User Access Team comprises well-established senior experts, several young researchers and an industrial partner (SME). The members of the proposing team have a leading role in ongoing efforts for the development of European standards for the design of FRP structures[10], for which the results of the project can provide essential knowledge. Such standards will support the market uptake of this innovative technology in the construction sector.

The test specimens consisted of 2-storey frames, with 2 longitudinal bays and a single transverse bay. The structures were made of pultruded GFRP profiles, with stainless-steel connections. Concrete precast slabs were installed on the GFRP beams creating the floors of the specimens, simulating the equivalent vertical loads of a real application, and allowing to anchor the actuators. The experimental campaign included the testing of four specimens: two without lateral bracings and two with such bracings. The modal identification of all specimens was performed using data of snap-back tests. For both types of frames, the first specimen was tested under monotonic loading, while the second underwent cyclic pseudo-static loading with increasing displacement amplitude. All tests were performed under displacement control. During the tests, the monitoring system recorded the applied loads and displacements, as well as rotations and strains of joints and members at key locations.

The experimental campaign

The experimental campaign consisted of sway tests of large-scale frame structures comprising pultruded GFRP profiles, as shown in Figure 1. The columns consisted of double-I section profiles (220×240×13 mm), and the longitudinal beams were made of two channel section profiles (200×60×10 mm). The transverse beams, on the other hand, consisted of I-shaped profiles (200×100×10 mm). Finally, in the braced frames, the bracings were made of angle (L-shaped) section profiles (100×60×10 mm).

Materials

The pultruded GFRP profiles used for the specimens were supplied by MM s.r.l. a Socio Unico, which is part of the User Assess Team. All profiles used are classified as “CE-A” quality (internal commercial reference[11]) and the mechanical properties reported by the manufacturer are presented in Table 1.

The connections between the columns and the footings (anchored to the laboratory’s strong floor) comprised two gusset plates (8 mm thickness) welded to a base plate (15 mm thickness), all made of 1.4301[12] (AISI 304[13]) stainless steel. The web cleated connections between the columns and the transverse beams were also produced by cold forming 6 mm thick 1.4301[12] stainless steel plates. The gusset and base plates connecting the columns to the bracings (braced specimens only) were made of 1.4301 stainless steel[12]. All connections between GFRP members were bolted using A2-70[14] grade stainless steel bolts, rods, washers and nuts. The column-to-footing connection plates were anchored to the footings with ϕ16 mm carbon steel rods, class 10.9[15].

A precast flooring system was installed on the GFRP frame specimens, materialized by C30/37[16] concrete and reinforced with carbon steel rebars class B450C[17]. It should be stressed that the concrete slabs are not part of the conceptual design of the specimens (in an actual all-composite structure, the floors would likely be made of composite sandwich panels), serving only as a mean to apply vertical (dead) and horizontal (connected to the actuator) loads without suffering any damage during the tests.

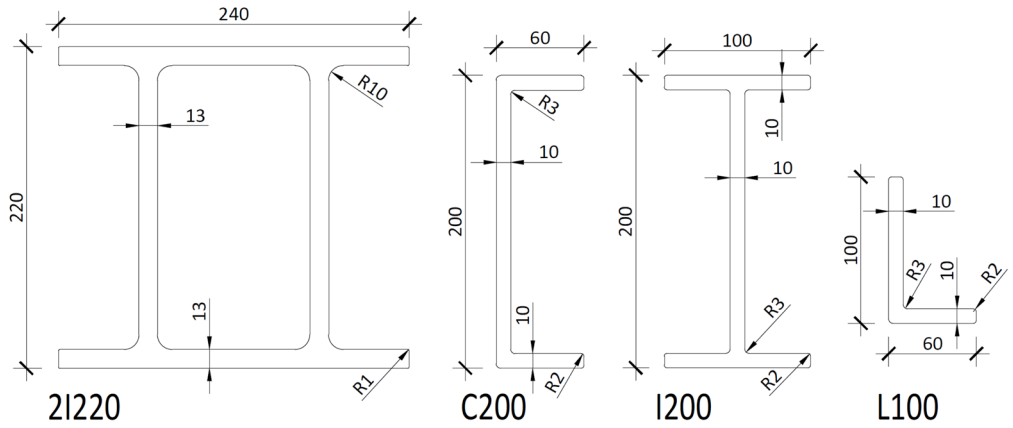

Figure 1. Cross-sections of the pultruded GFRP profiles used in the tests (dimensions in mm).

Table 1. GFRP material properties[11].

Loading	Property	Direction	Symbol	Values		Unit
				Average	Characteristic	
In-plane tension	Modulus	Longitudinal	$E_{x,t}$	33.1	-	GPa
		Transverse	$E_{y,t}$	11.8	-	
	Strength	Longitudinal	$f_{x,t}$	470	451	MPa
		Transverse	$f_{y,t}$	90.1	84.6	
	Poisson's ratio	Major	υ_{xy}	0.30	-	-
		Minor	υ_{yx}	0.10	-	
In-plane compression	Modulus	Longitudinal	$E_{x,c}$	30.0	-	GPa
		Transverse	$E_{y,c}$	11.1	-	
	Strength	Longitudinal	$f_{x,c}$	393	374	MPa
		Transverse	$f_{y,c}$	127	115	
Flexure	Strength	Longitudinal	$f_{x,f}$	494	472	MPa
		Transverse	$f_{y,f}$	217	185	
Interlaminar shear	Strength	Longitudinal	$f_{xz,ILS}$	25.1	21.3	MPa
Pin-bearing	Strength	Longitudinal	$f_{x,br}$	225	200	MPa
		Transverse	$f_{y,br}$	155	122	

Test specimens

Four specimens were tested in the experimental campaign, as summarized in Table 2. The specimens can be divided in two configuration categories - (i) braced and (ii) unbraced - and in two test categories - (a) monotonic and (b) pseudo-static cyclic loading (henceforth referred to as "cyclic").

All specimens had the same overall geometry, detailed in the next subsection, with specimens BFrame-M and BFrame-C containing a lateral bracing system.

Table 2. List of test specimens.

Specimen	Bracings	Loading
uFrame-M	No	Monotonic
uFrame-C	No	Cyclic
BFrame-M	Yes	Monotonic
BFrame-C	Yes	Cyclic

Geometry of the specimens. Figure 2 shows the lateral elevation view of an unbraced specimen. The GFRP frames comprised two longitudinal bays, with 3913 mm between column axes. The total height of the columns was 6750 mm, with the axis of the 1st storey beams being positioned at 3200 mm from the bottom of the columns, and the 2nd storey beams positioned at 6400 mm.

Figure 3 illustrates the side view of the specimens, showing the single transverse bay with 2000 mm between the column axes.

Figure 4 and Figure 5 show the plan view of specimens with and without the slabs installed. The latter figure includes the position of the slab connectors, whose geometry is detailed ahead in this document.

As mentioned, the column-to-footing connections, depicted in Figure 6, comprised double-gusset plates welded to a base plate.

The connections between the columns and the longitudinal beams did not comprise auxiliary parts, with both members being directly bolted to each other. To that end, at the beam and column intersections, the flanges of the columns were locally cut, as depicted in Figure 7, leaving a 10 mm gap between the flanges of the columns and the flanges of the webs.

On the other hand, the connections between the columns and the transverse beam, detailed in Figure 8, comprised stainless steel web cleats.

The bracing system installed in specimens BFrame-M and BFrame-C, illustrated in Figure 9, comprised L100 profiles (*cf.* Figure 1) connected to the columns, using metallic auxiliary parts, comprising a gusset plate welded to a base plate. Figure 10 presents the details of these connections.

Regarding the concrete slabs, as mentioned, they were not a part of the structural system under testing, but a part of the test setup, simulating the vertical loads, and allowing to introduce the lateral loads. In this context, each slab floor was divided in four precast modules, two interior ones and two lateral ones, shown in Figures 11a and 11b, respectively. The design of the slabs guaranteed that there was no concrete-GFRP composite action in the vicinity of the supports, and that the slabs did not transmit bending moments from one span to the other.

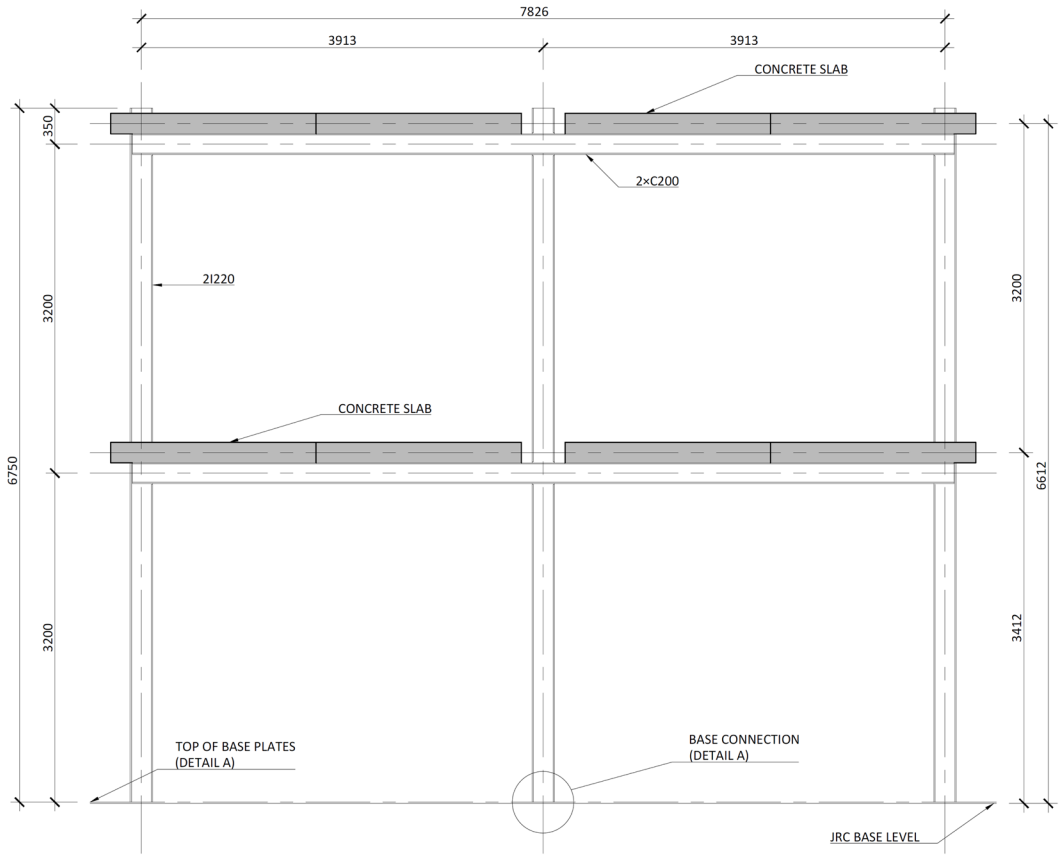

Figure 2. Elevation view of unbraced specimens (dimensions in mm).

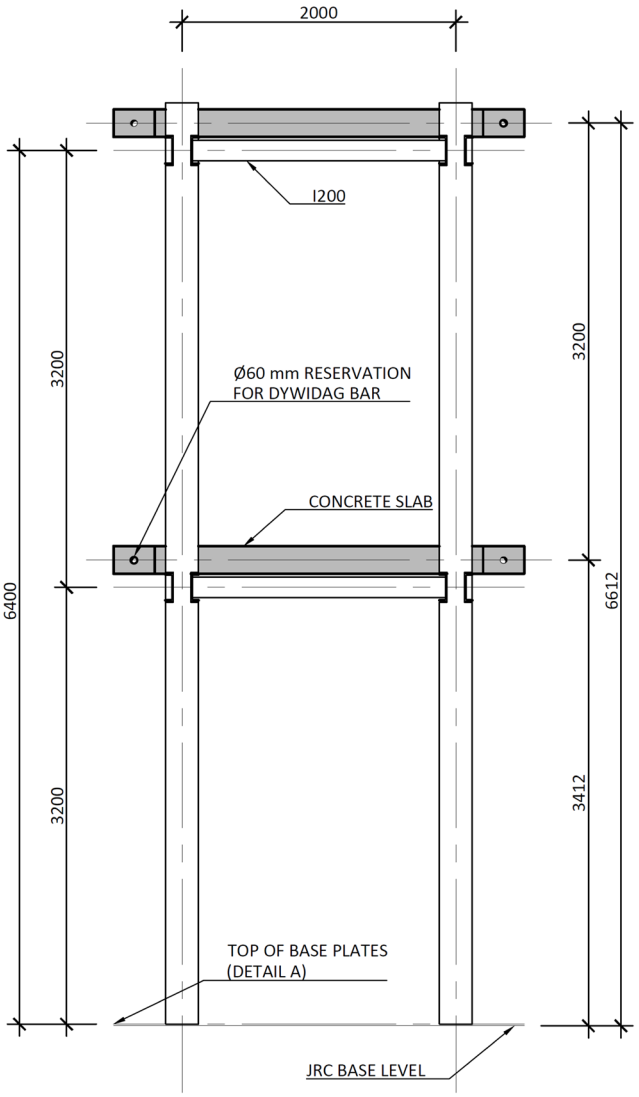

Figure 3. Side view of specimens (dimensions in mm).

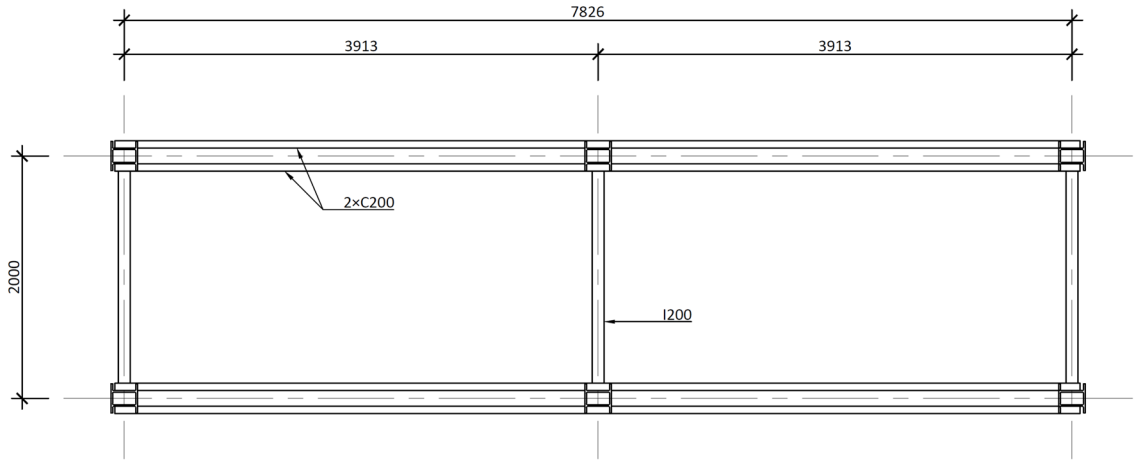

Figure 4. Plan view of specimens without floor slabs (dimensions in mm).

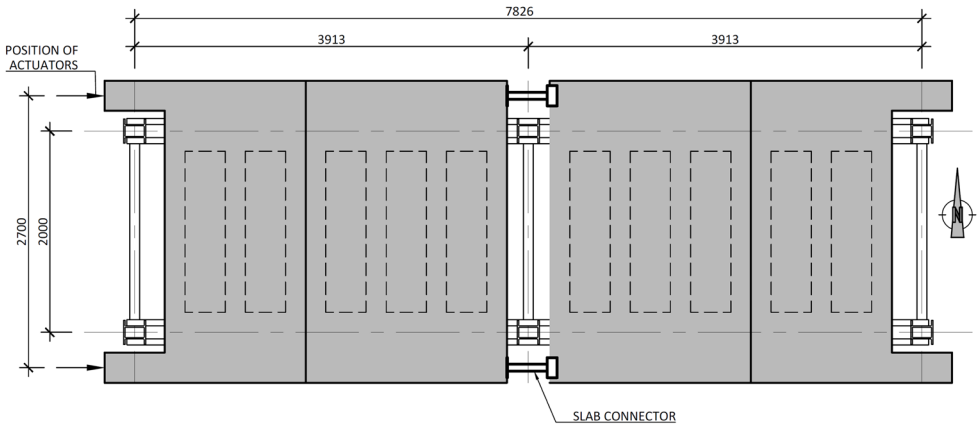

Figure 5. Plan view of specimens with floor slabs (dimensions in mm).

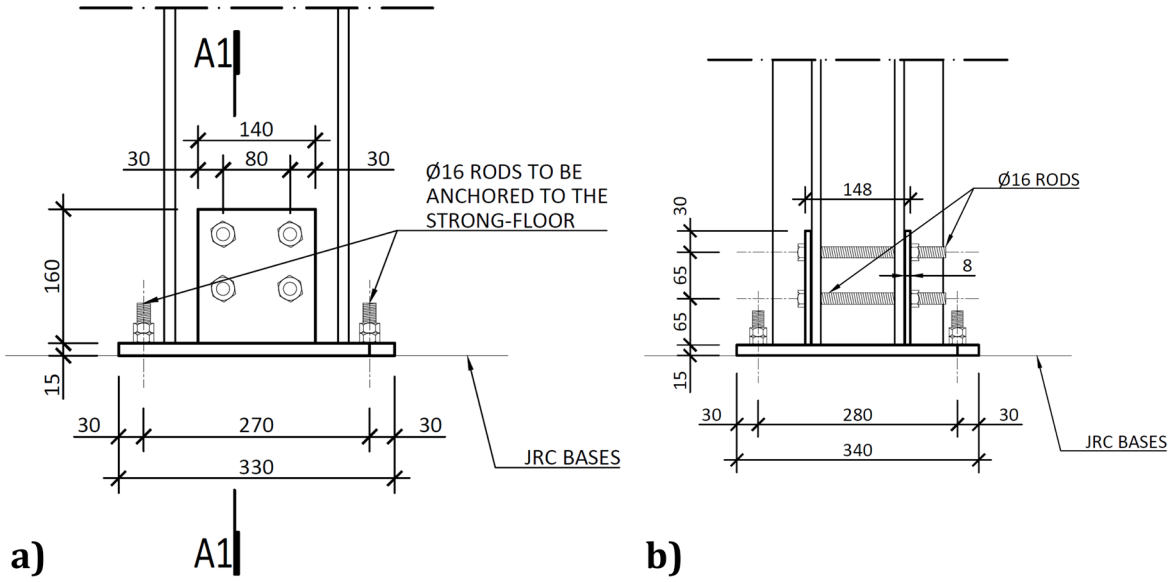

Figure 6. Column-to-footing connections: **a**) detail A (*cf.* Figure 2); and **b**) section A1-A1 (dimensions in mm).

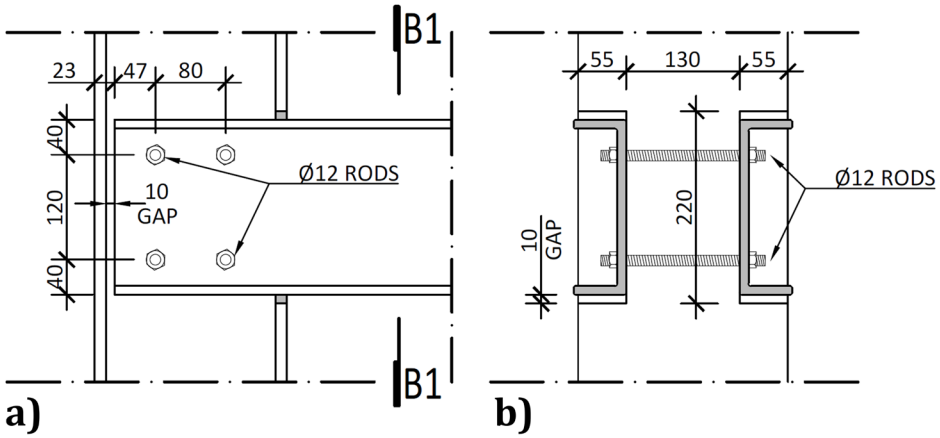

Figure 7. Longitudinal beam to column connections: **a**) external side view; and **b**) section B1-B1 (dimensions in mm).

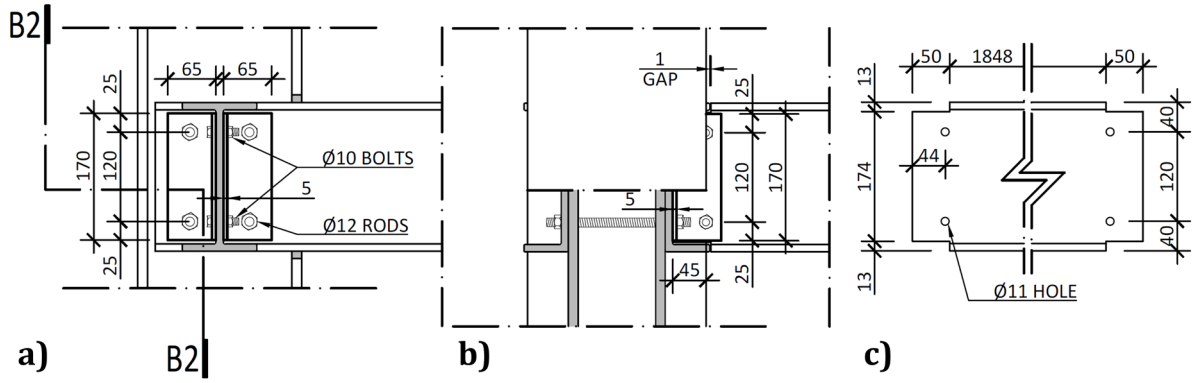

Figure 8. Transverse beam-to-column connections: **a**) internal side view; **b**) section B2-B2; and **c**) geometrical details of transverse beams (dimensions in mm).

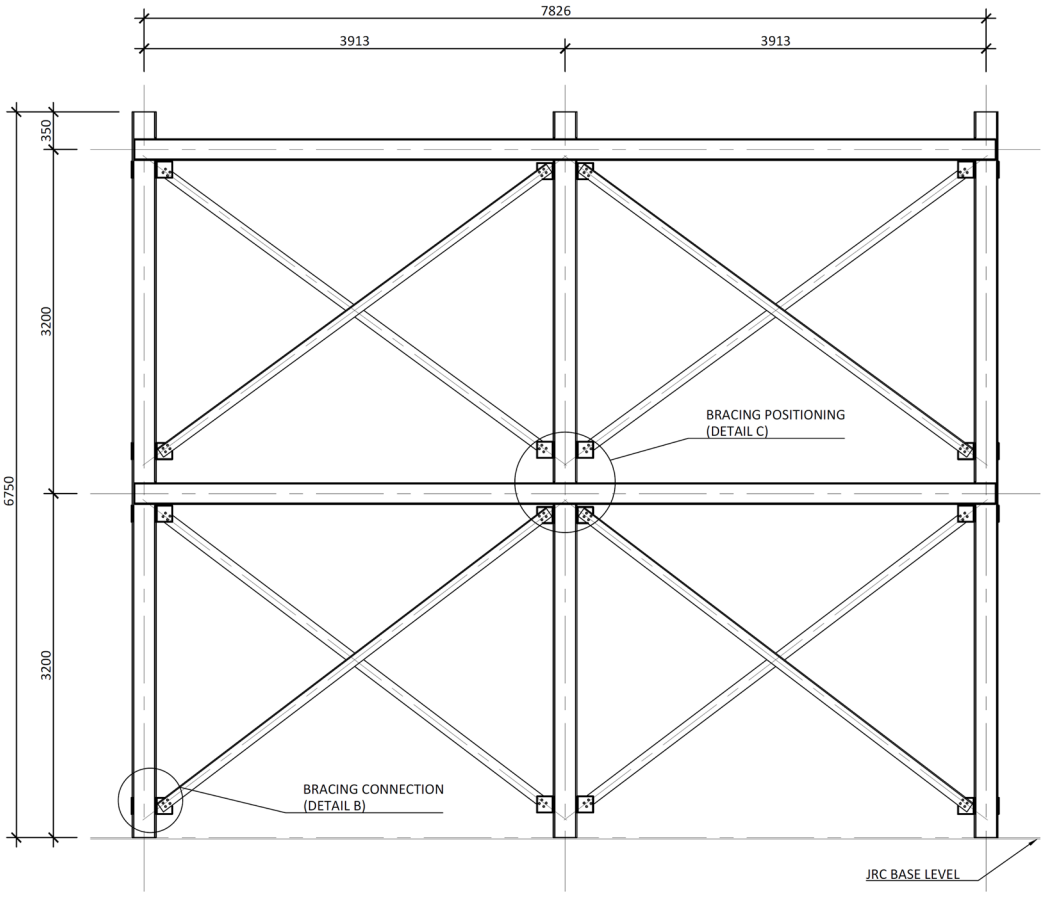

Figure 9. Elevation view of braced specimens, without slabs (dimensions in mm).

The nominal overall thickness of the slabs was 200 mm, and expanded polystyrene blocks were used as lost formwork to decrease the overall weight of the slabs, as shown in Figure 12. Moreover, slab overhangs, depicted in Figure 13, were provided on both sides of the frame, which also extended longitudinally beyond the GFRP frame. The actuators applied the horizontal loads to these overhangs. Reservations with 60 mm diameter were installed in the overhangs, allowing the installation of *Dywidag* bars used to reverse the loading during the cyclic tests. Overall, the nominal mass of the interior

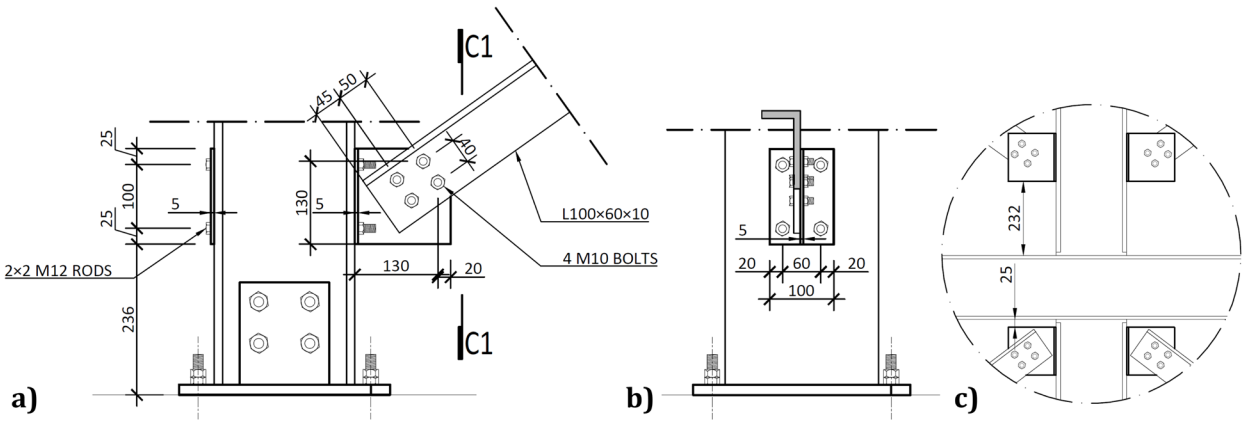

Figure 10. Bracing-to-column connections: **a**) detail B (*cf.* Figure 9); **b**) section C1-C1; and **c**) Detail C (dimensions in mm).

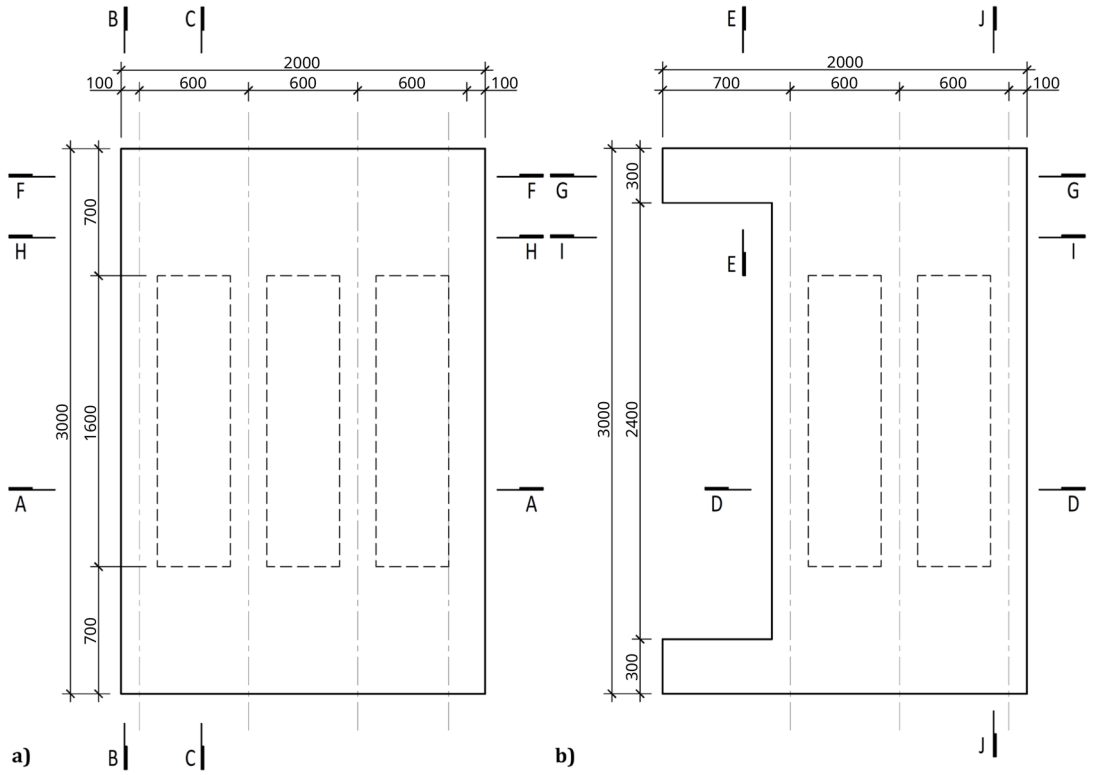

Figure 11. Floor slab parts: **a**) interior part; **b**) exterior part (dimensions in mm).

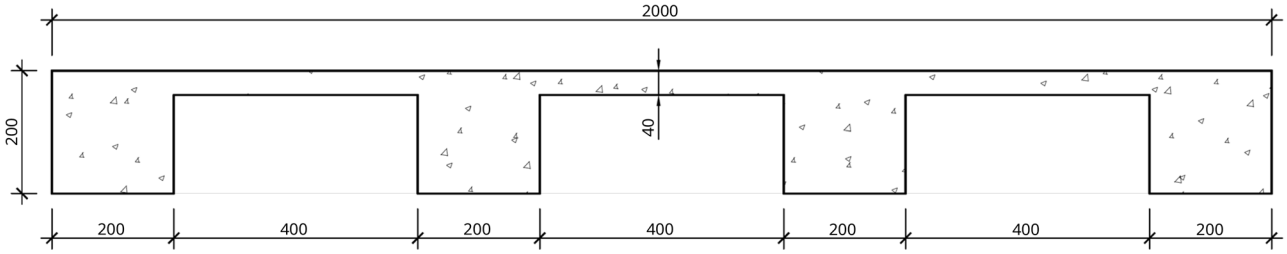

Figure 12. Floor slabs: section A-A, *cf.* Figure 11 (dimensions in mm).

slabs was 2275 kg, while the exterior slabs add a nominal mass of 1802 kg.

The slabs were internally reinforced with steel rebars. Figure 14 to Figure 16 show the reinforcement detailing according to the sections identified in Figure 11.

The slab-beam shear connections comprised *TECNOGRIP* anchors[18], a system developed for precast concrete structures. To that end, anchor channel 40/22/2.5[18] metallic elements were installed in the slabs, during the casting, as shown in Figure 17. After the positioning of the slabs over the frame structure, the shear connection was completed by attaching

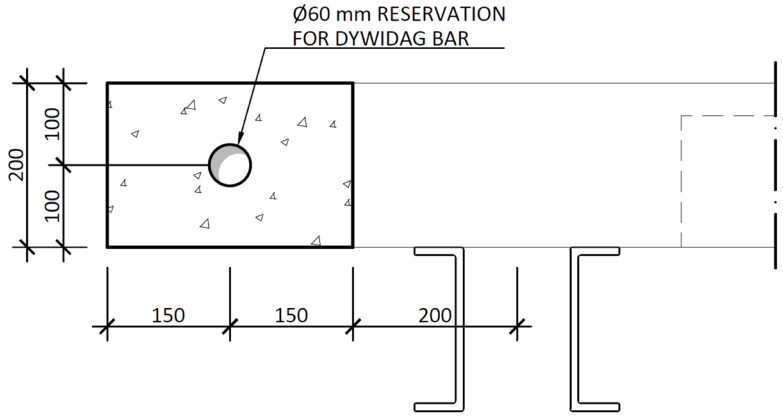

Figure 13. Floor slabs: section E-E, *cf*. Figure 11 (dimensions in mm).

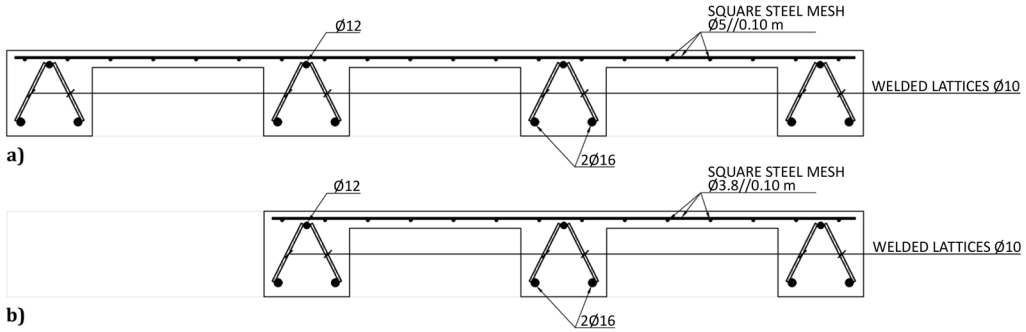

Figure 14. Reinforcement detailing of slabs: **a**) section A-A and **b**) section D-D (*cf*. Figure 11).

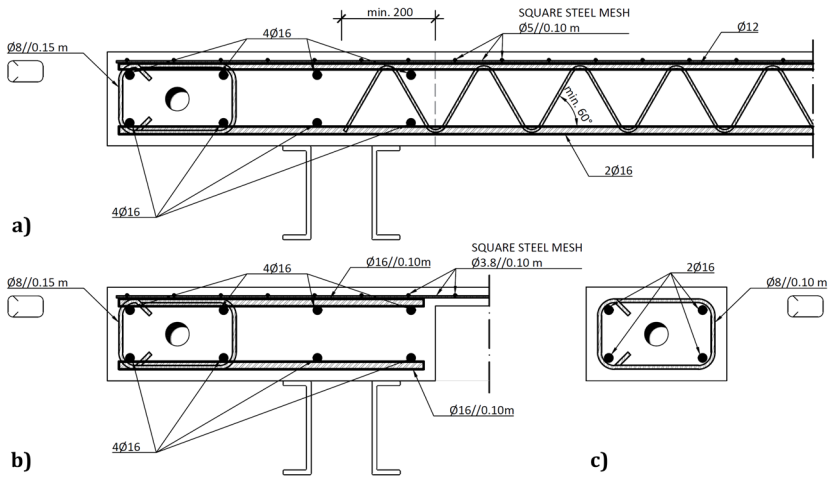

Figure 15. Reinforcement detailing of slabs: **a**) section B-B, **b**) section C-C and **c**) section E-E (*cf*. Figure 11).

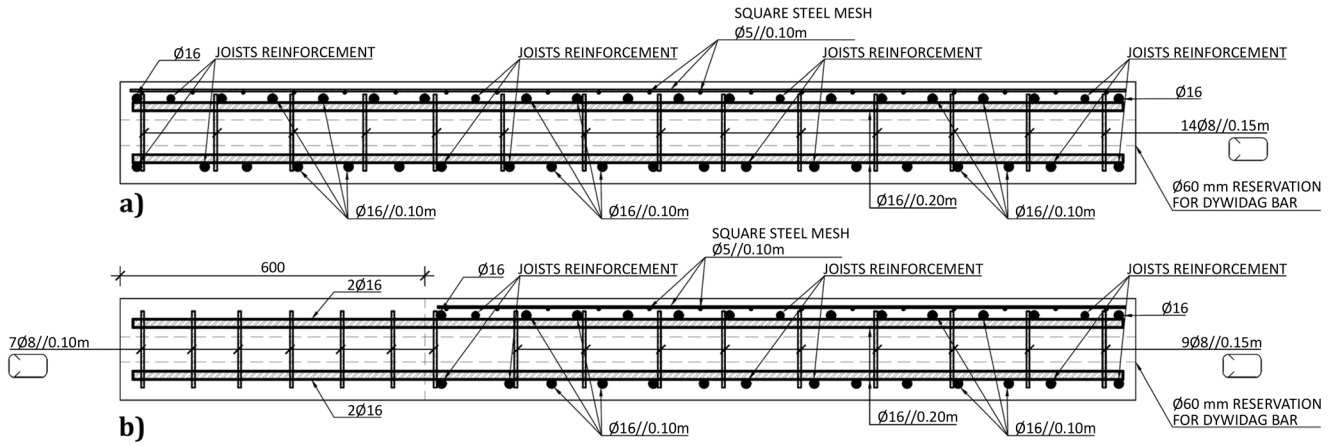

Figure 16. Reinforcement detailing of slabs: **a**) section F-F, and **b**) section G-G (*cf.* Figure 11).

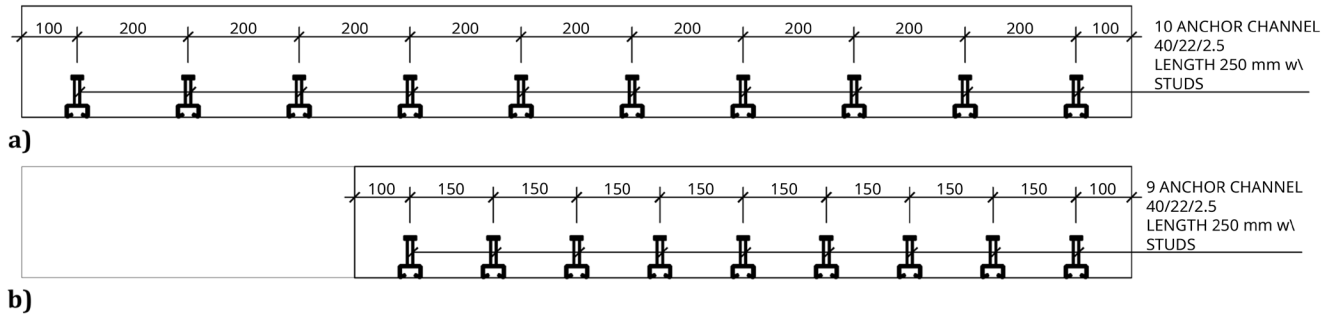

Figure 17. Shear connection detailing: **a**) section H-H, and **b**) section I-I, *cf.* Figure 11 (dimensions in mm).

a companion steel part to the anchor channels, which were then bolted to the beams, as shown in Figure 18.

Finally, the slab connector depicted in Figure 5 comprised a steel (grade S235) CHS tube, to be aligned with the slabs reservations, allowing the installation of the *dywidag* bars, welded to top plates. Figure 19 presents the details of these elements, which allowed for the prestressing of the *dywidag* bars, required to reverse the loading in the cyclic tests.

Construction phases. The construction of the specimens began with the preparation of the individual structural members in MM's plant. This included the cutting to size of beam, column and bracing members, the drilling of the holes for the beam-to-column, column-to-footing and bracing-to-column connections, and the local cutting of the columns' flanges near the beam-to-column connections (*cf.* Figure 7). The preparation activities also included installing base plates for the inclinometers (*cf.* Section Set-up and instrumentation) and most of the strain gauges (some were installed later in the laboratory).

The structural members were then transported to the JRC ELSA facilities, along with the metallic connection parts and the precast slabs, which were outsourced by MM.

At the ELSA facilities, the specimen construction process was as follows:

1. Attachment of the base plate double gussets to the base plates (already anchored to the floor, Figure 20);
2. Positioning of the columns and bolting to the base plates (Figure 21);
3. Installation of the longitudinal beams in the 1st storey (Figure 22);
4. Installation of the transverse beams in the 1st storey (Figure 23);
5. Installation of wood rafters at quarters of the beams span[a] (Figure 23 and Figure 24);

[a] The objective of the wooden rafters was to increase the beams' torsional stiffness, avoiding lateral-torsional buckling (LTB). In the first specimen (uFrame-M), this step was skipped leading to the occurrence of LTB deformations in the beams when the slabs were installed (step 7). When these deformations were observed, the slabs were temporarily propped to the floor to install the wooden rafters. The deformations of the beams recovered completely, and no signs of damage were observed.

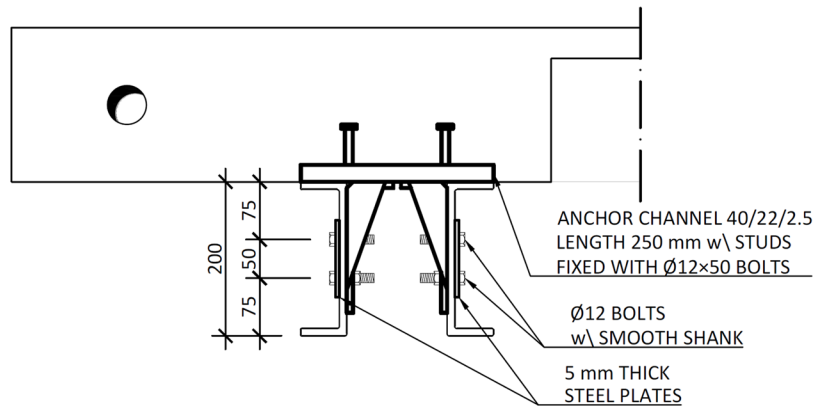

Figure 18. Shear connection detailing: section C-C, *cf*. Figure 11 (dimensions in mm).

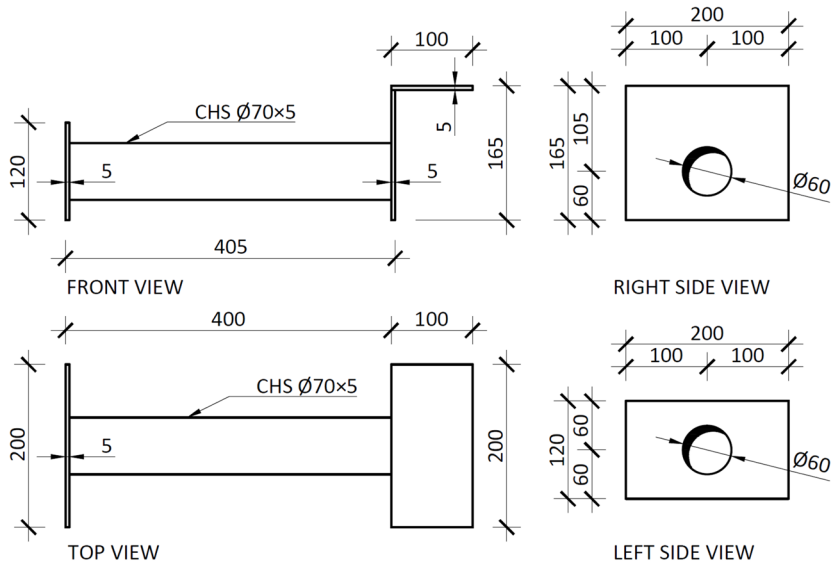

Figure 19. Slab connector (dimensions in mm).

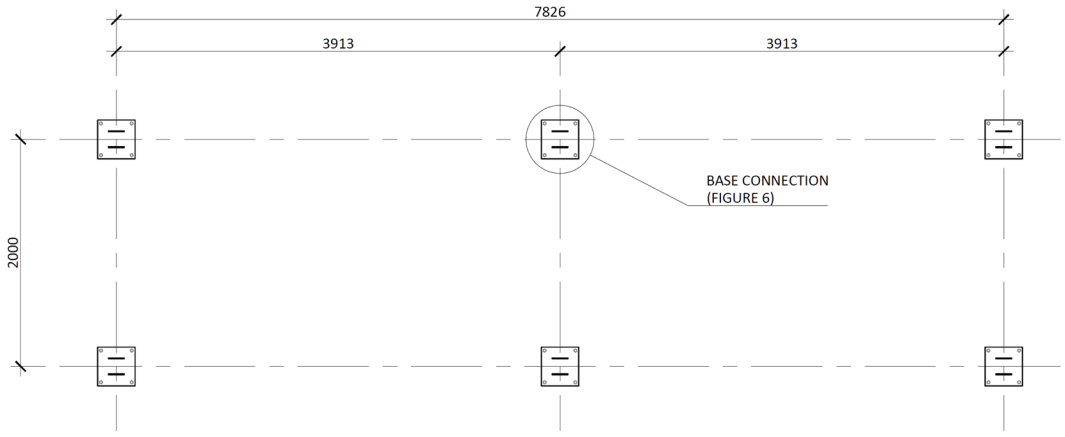

Figure 20. Installation of column-to-footing connection plates (dimensions in mm).

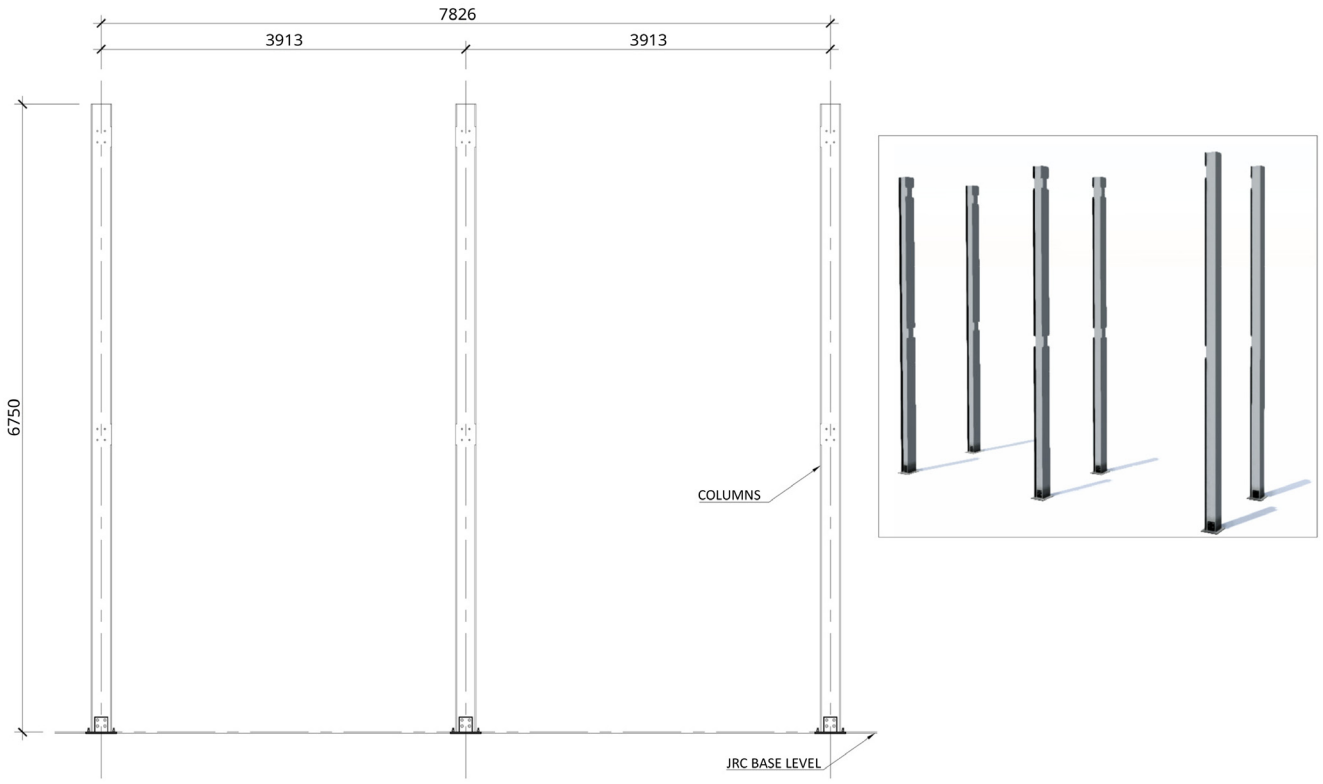

Figure 21. Installation of columns (dimensions in mm).

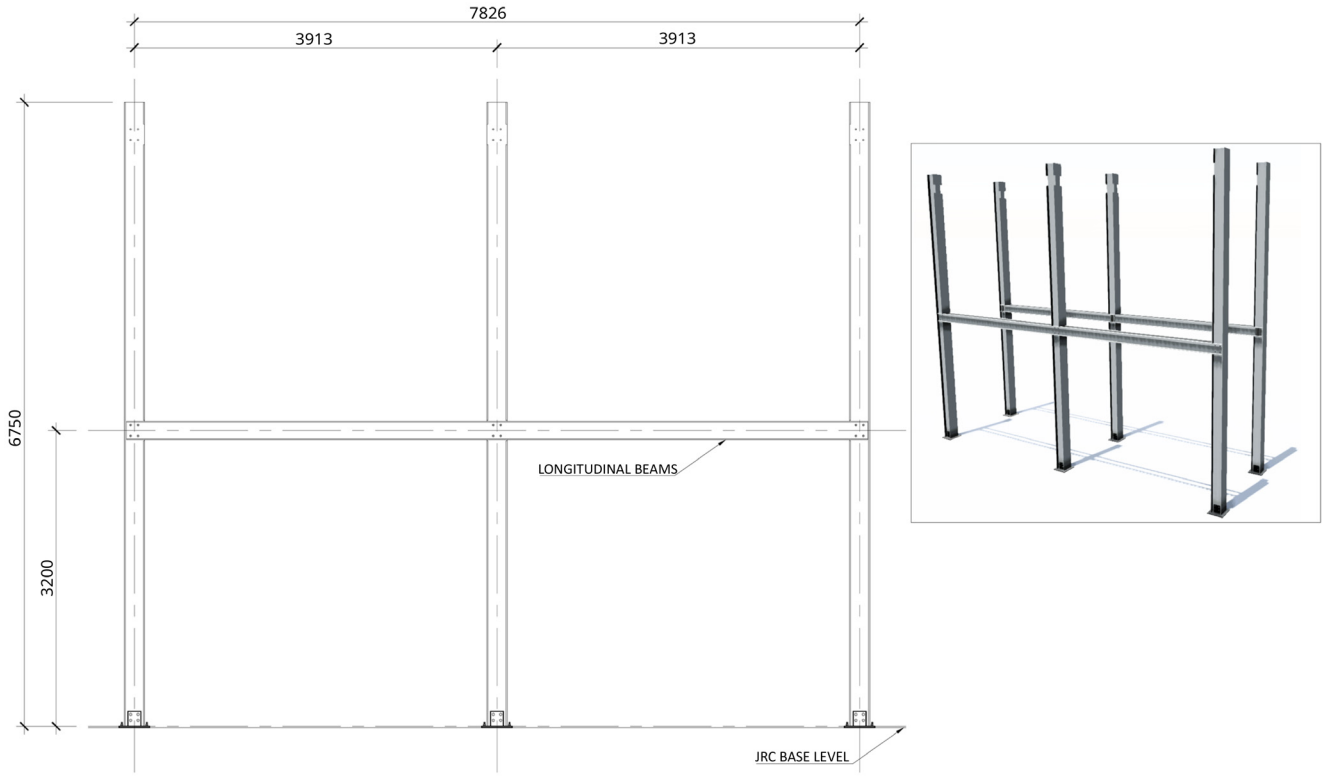

Figure 22. Installation of 1st storey longitudinal beams (dimensions in mm).

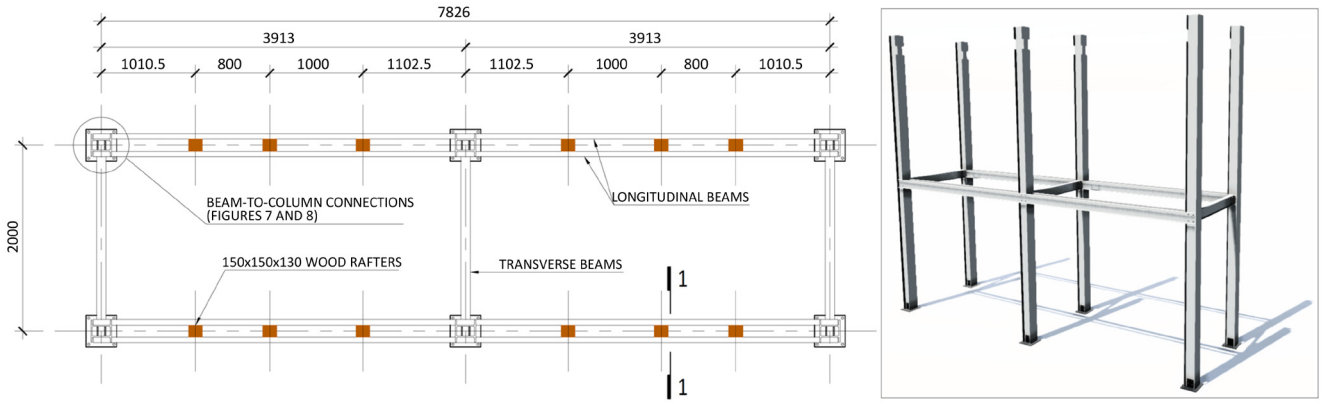

Figure 23. Installation of 1st storey transverse beams and wood rafters (dimensions in mm).

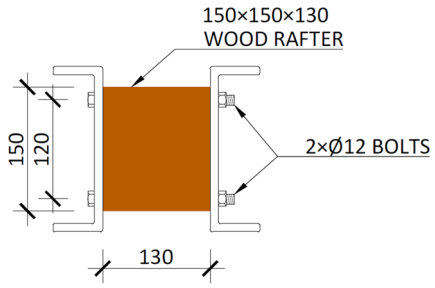

Figure 24. Detail of the wood rafters installed in beams (dimensions in mm).

6. Placement of the precast slabs over the 1st storey beams, including the *dywidag* bars, connecting steel plates and slab connectors (Figure 25 and Figure 26);

7. Installation of the shear connectors (*cf.* Figure 18) in the 1st storey slabs, without fastening to the beams (Figure 27);

8. Installation of the longitudinal beams in the 2nd storey (Figure 28);

9. Installation of the transverse beams in the 2nd storey (Figure 29);

10. Installation of wood rafters at quarters of the beams span in the 2nd storey;

11. Placement of the precast slabs over the 2nd storey beams, including the *Dywidag* bars, connecting steel plates and slab connectors (Figure 30);

12. Installation of the shear connectors (*cf.* Figure 18) in the 2nd storey slabs, without fastening to the beams;

13. Application of prestress to the *Dywidag* bars;

14. Installation of the bottom bracings (Figure 31, specimens BFrame-M and BFrame-C only);

15. Installation of the top bracings (Figure 32, specimens BFrame-M and BFrame-C only);

16. Fastening of the shear connectors to the beams (*cf.* Figure 18 and Figure 27), including drilling of the holes in the beams, and installation of the external steel strengthening plates (Figure 33, not used in specimen uFrame-M).

It should be mentioned that for the first specimen, uFrame-M, step 16 was performed before step 13. This led to the occurrence of some damage on the shear connection system, namely the ovalisation of the beams bolt holes, which was not detected before the tests due to the presence of the washers. As a consequence, as described ahead in this paper, that particular specimen presented an asymmetric response from the onset of the test, also exhibiting sliding between the slabs and the frame. Owing to this unwanted behaviour, in the remaining specimens, the sequence of the mounting operation was modified according to what was previously described.

Set-up and instrumentation

As mentioned, the experimental campaign focused on sway tests of large-scale GFRP frame structures. Figure 34 presents a scheme of the test setup, showing the nomenclature of the load application points and of the columns. The reaction wall was located on the West side of the specimens. In the opposite side (*i.e.*, the East side), the horizontal displacements were measured at both the columns and the slabs. The loads were applied by 4 actuators, with a capacity of 500 kN and total stroke of 500 mm. The loads were measured by load cells built-in the actuators (*Maywood* 500 kN). The horizontal displacements were also measured by the built-in digital sensors of the actuators (*Temposonics*) positioned on the West side of the specimens. Additionally, 8 sensors (linear encoders, *Heidenhain MSA 375*) on the East side of the specimens were used to measure the displacements of the concrete slabs and the composite columns. This also allowed evaluating possible slip deformations due to the potential flexibility of the shear connections. Please note that the calibration reports of force

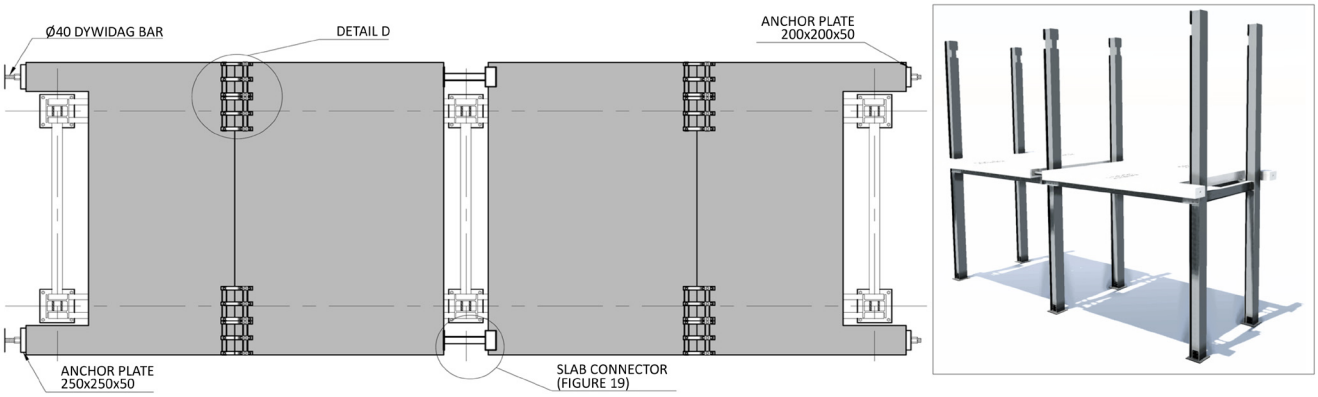

Figure 25. Placing of 1st storey slabs, installation of connecting plates and slab connectors (dimensions in mm).

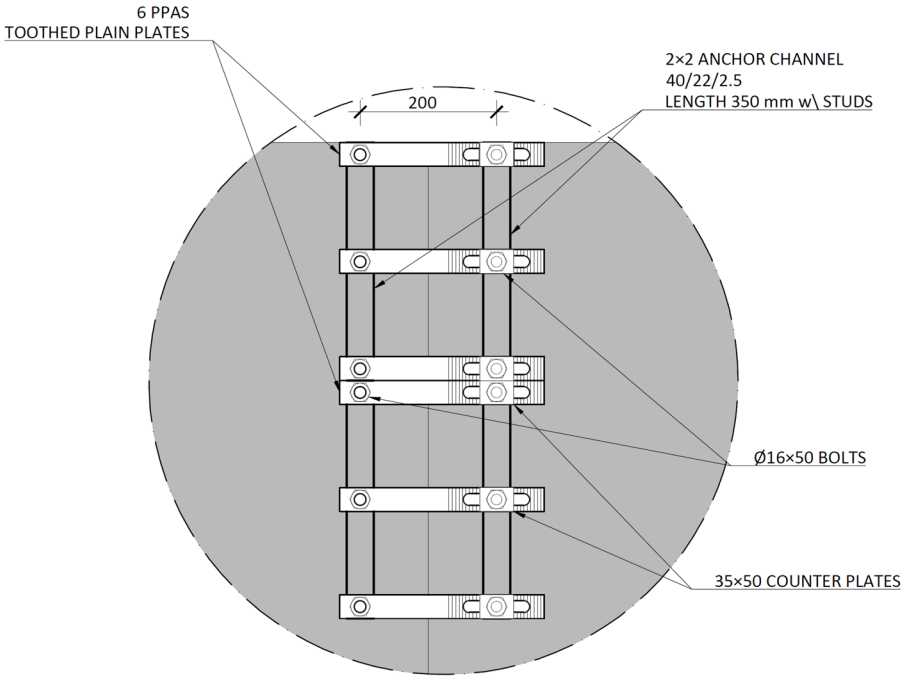

Figure 26. Connecting plates – Detail D (dimensions in mm).

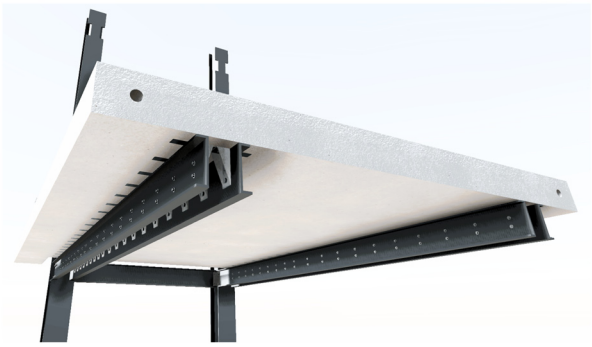

Figure 27. Illustration of the shear connectors configuration on the 1st storey slabs.

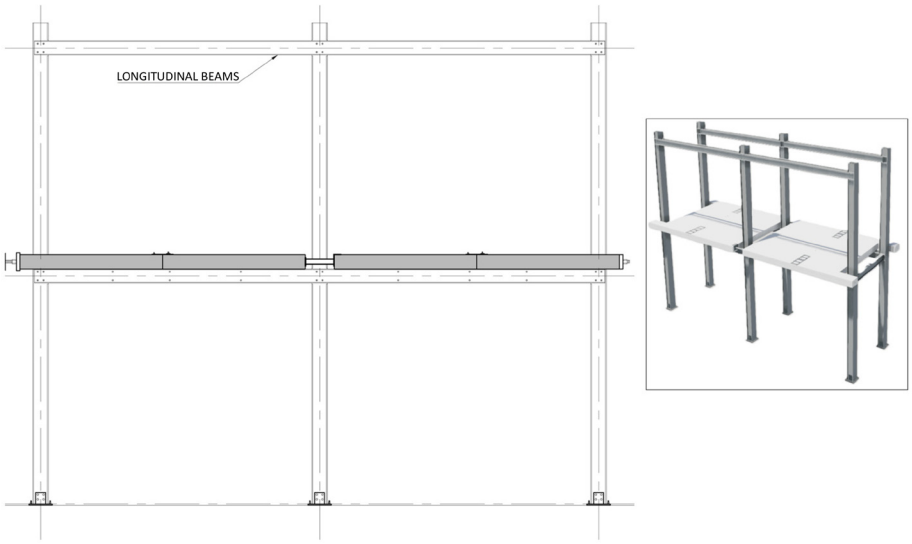

Figure 28. Installation of 2nd storey longitudinal beams.

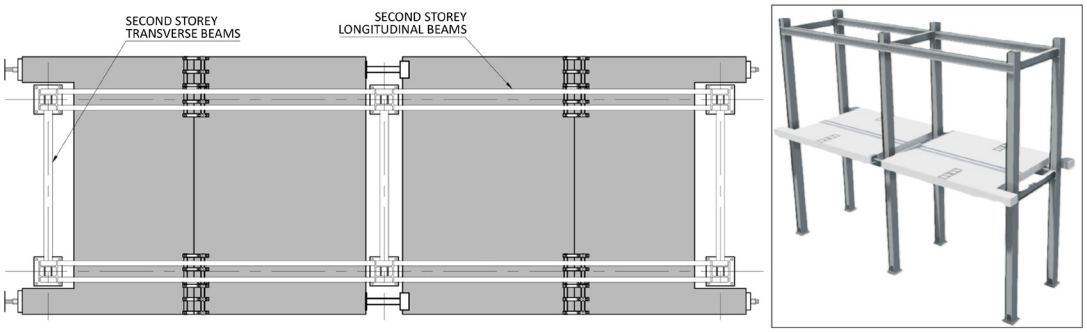

Figure 29. Installation of 2nd storey transverse beams.

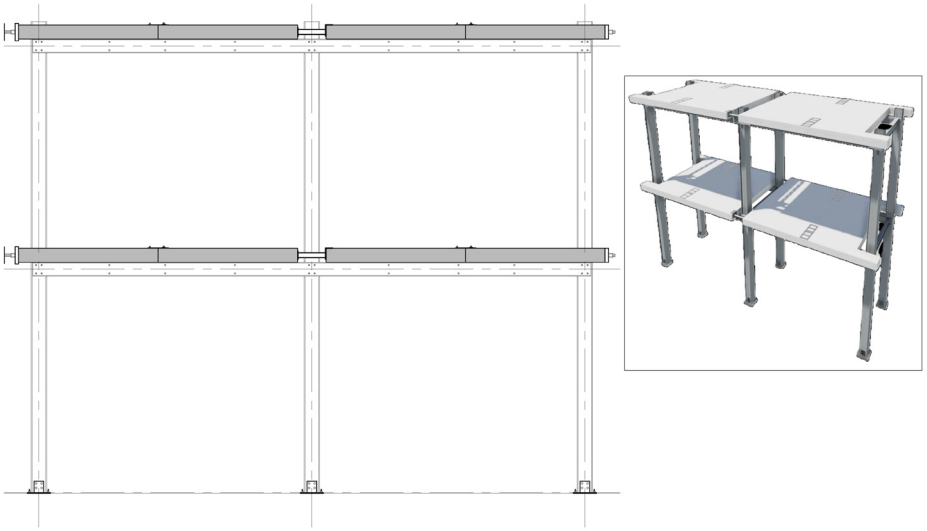

Figure 30. Placing of 2nd storey slabs, installation of connecting plates and slab connectors.

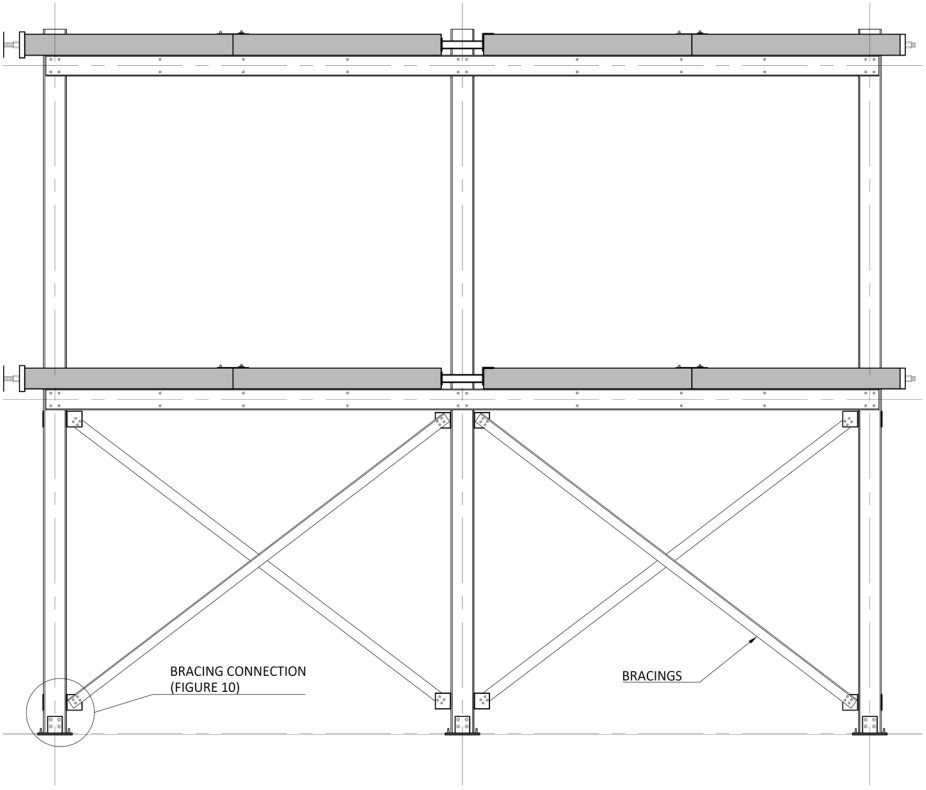

Figure 31. Installation of the bottom bracings (only for BFrame-M and BFrame-C).

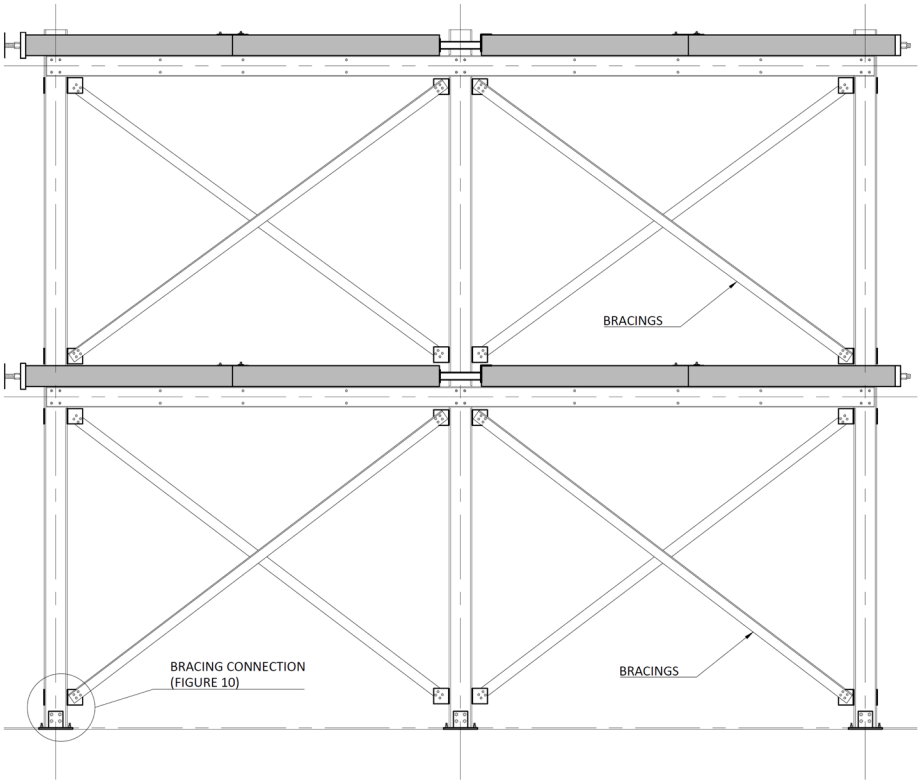

Figure 32. Installation of the top bracings (only for BFrame-M and BFrame-C).

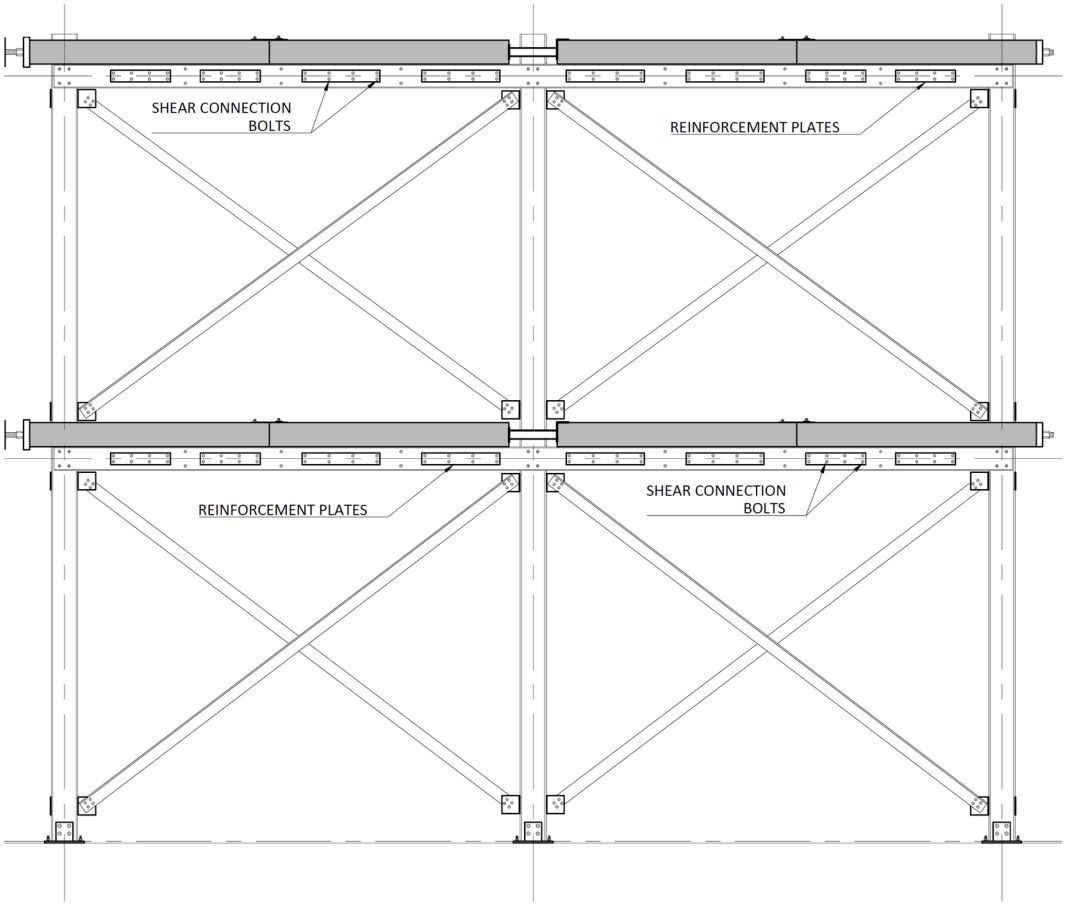

Figure 33. Installation of the shear connectors in the beams (bracings only for BFrame-M and BFrame-C).

and displacement sensors are included in the dataset. For additional details about the interpretation of the calibration reports, the reader can refer to the Technical Report No JRC139347[19]. Figure 34 shows a schematic tri-dimensional view of the specimens, indicating their position with respect to the compass, also showing the numbering of the load measuring equipment and the nomenclature of the columns. Regarding the nomenclature of the displacement measurements, the slab displacements on the West side are identified by Con, while, on the East side, the slab and column displacements are identified as HS and HC, respectively. The numbering of the displacement transducers follows the same distribution adopted for the applied loads (*cf.* Figure 34).

The rotations of the columns and beams were measured in the vicinity of the beam-to-column connections, with inclinometers from *SEIKA* (model *SBU1*), with stroke of ±5°, installed as depicted in Figure 35. The column inclinometers were positioned under the longitudinal beams, at ~ 200 mm from their mid-axis, and named *CR-Level-Column-U*, where *Level* refers to the storey (1 or 2) and the *Column* also identifies the longitudinal lateral frame, *i.e.*, A1 refers to column A (*cf.* Figure 34) of the South lateral frame (1), while A2 refers to column A of

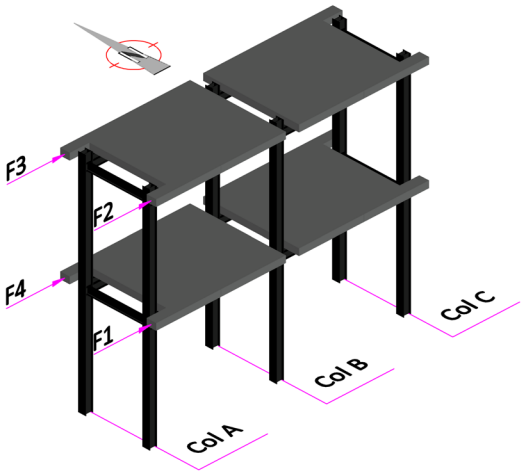

Figure 34. Tri-dimensional schematic view of specimens, including orientation and load and column numbering.

the North lateral frame (2). U simply highlights that the inclinometer is placed under the beam. As an example, CR-2-B1-U refers to the inclinometer placed in column B of the South

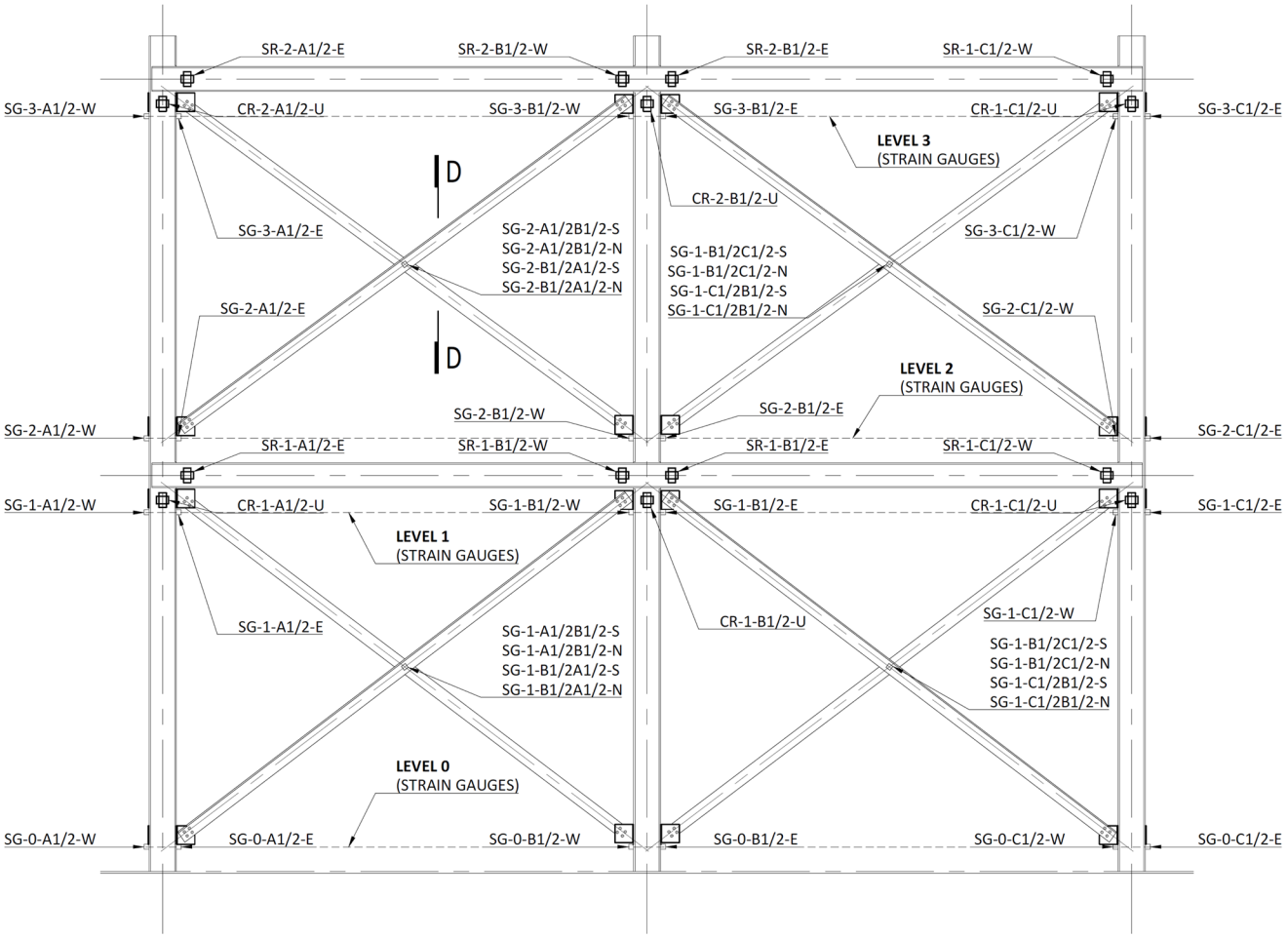

Figure 35. Positioning of the inclinometers and strain gauges in South (1) and North (2) lateral frames.

lateral frame under the 2nd storey beam. Similarly, the beam inclinometers were named *SR-Level-Column-Side*, where *Level* refers to the storey (1 or 2), *Column* includes the identification of the lateral frame and, in this case, *Side* indicates if the inclinometer is positioned in the West (W) or East (E) side of the column. For instance, SR-1-B2-W refers to the inclinometer positioned at the West side of the column B of the North frame's 1st storey. It should be mentioned that the beam inclinometers were positioned at ~200 mm from the vertical axis of the columns.

Figure 35 also depicts the positions of the strain measurement points on the columns and on the bracings. Electric strain gauges from TML, models FLKB-6-11-3LJC-F or FLA-6-11 were used. For the columns, two strain gauges were used per section, positioned at the mid-width of both flanges. The measurements were made at 4 levels: at distances of ~200 mm (0), ~2900 mm (1), ~3500 mm (2), and 6100 mm (3) from the bottom of the column profiles. The measuring points were named *SG-Level-Column-Side*, in which the *Column* also includes the indication of the lateral frame (1 for South and 2 for North), while the *Side* indicates the strain gauge bonded on the West (W) or East (E) flange of the respective column.

For the bracings, the strain gauges were installed in the vicinity of mid-span, on both sides of the longer angle leg, as exemplified in Figure 35 and Figure 36. The measuring positions were named *SF-Level-Bottom column/Top column-Side*. In this case, the *Level* refers to the bracings of the first (1) or second (2) storey, respectively. *Bottom column* refers to the column to which the bracing has its lower connection, while the *Top column* identifies the column to which it has its upper connection, while *Side* refers to the position of the strain gauge in the bracings section (South or North, *cf.* Figure 36). As an example, SG-1-C2B2-N refers to the strain gauge positioned at the bottom storey (1) of the North lateral frame (2), connecting the bottom of column C2 to the top of column B2, on the North side.

Table 3 and Table 4 present the complete list of the measurements made, including the type of measurement, the position, and the specimens for which measurements were taken.

During the tests, ELSAREC, the ELSA REal-time Controller (for further details, refer to 20), was used to monitor the response of the specimens: as also described in the Technical Report No JRC141264[19], multiple acquisitions run in parallel. During the snap-back tests used for the dynamic identification of the specimens, the signals from the monitoring system were recorded at a rate of 1000 Hz. On the other hand, during the sway tests, the signals of the standard instruments (*e.g.*, inclinometers and strain gauges) were acquired at 10 Hz, while the signals from the control system (*e.g.*, control variables) were sampled at a variable rate. These last signals were recorded at the achievement of each record of the loading pattern, noting that the prototype-time variable common to both acquisition files can be used for synchronisation purposes. Furthermore, during the sway tests, the readings of some additional strain gauges were recorded by another datalogger, model *QuantumX* from *HBM*, sampling at a rate of 1 Hz, and the results were synchronised through a trigger input signal.

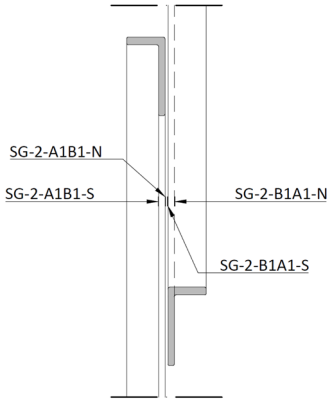

Figure 36. Section D-D (*cf.* Figure 35): positioning of bracing strain gauges at South (1) frame.

Test programme and loading input

The main objective of the experimental campaign was to perform sway-tests on the specimens. Before and after the sway tests, all the specimens were subjected to snap-back tests, in which a load was applied at F1 location (*cf.* Figure 34) using a fuse. After the fuse broke, the free vibration of the structures was measured through their displacements on the East side. These results were then used to estimate the vibration frequencies before and after the sway tests.

The following Table 5 reports the lists of the experiments, including both dynamic identification and quasi-static sway tests, performed on the four specimens.

The sway tests were conducted under displacement control. The monotonic tests were performed at a rate of 12 and

Table 3. List of load, displacement and rotation measurements.

Type	Nomenclature	Frame	Level	Position	Specimens
Load	F1	South	1st storey	Slab, near A1	All
	F2	South	2nd storey	Slab, near A1	All
	F3	North	1st storey	Slab, near A2	All
	F4	North	2nd storey	Slab, near A2	All
Displacement	Con1	South	1st storey	Slab, near A1	All
	Con2	South	2nd storey	Slab, near A1	All
	Con3	North	1st storey	Slab, near A2	All
	Con4	North	2nd storey	Slab, near A2	All
	HS1	South	1st storey	Slab, near C1	All
	HS2	South	2nd storey	Slab, near C1	All
	HS3	North	1st storey	Slab, near C2	All
	HS4	North	2nd storey	Slab, near C2	All
	HC1	South	1st storey	C1	All
	HC2	South	2nd storey	C1	All
	HC3	North	1st storey	C2	All
	HC4	North	2nd storey	C2	All

Type	Nomenclature	Frame	Level	Position	Specimens
Rotation	CR-1-A1-U	South	1st storey	A1	All
	SR-1-A1-E	South	1st storey	Beam, East of A1	All
	CR-1-B1-U	South	1st storey	B1	All
	SR-1-B1-W	South	1st storey	Beam, West of B1	All
	SR-1-B1-E	South	1st storey	Beam, East of B1	All
	CR-1-C1-U	South	1st storey	C1	All
	SR-1-C1-W	South	1st storey	Beam, West of C1	All
	CR-2-A1-U	South	2nd storey	A1	All
	SR-2-A1-E	South	2nd storey	Beam, East of A1	All
	CR-2-B1-U	South	2nd storey	B1	All
	SR-2-B1-W	South	2nd storey	Beam, West of B1	All
	SR-2-B1-E	South	2nd storey	Beam, East of B1	All
	CR-2-C1-U	South	2nd storey	C1	All
	SR-2-C1-W	South	2nd storey	Beam, West of C1	All
	CR-1-A2-U	North	1st storey	A2	All
	SR-1-A2-E	North	1st storey	Beam, East of A2	All
	CR-1-B2-U	North	1st storey	B2	All
	SR-1-B2-W	North	1st storey	Beam, West of B2	All
	SR-1-B2-E	North	1st storey	Beam, East of B2	All
	CR-1-C2-U	North	1st storey	C2	All
	SR-1-C2-W	North	1st storey	Beam, West of C2	All
	CR-2-A2-U	North	2nd storey	A2	All
	SR-2-A2-E	North	2nd storey	Beam, East of A2	All
	CR-2-B2-U	North	2nd storey	B2	All
	SR-2-B2-W	North	2nd storey	Beam, West of B2	All
	SR-2-B2-E	North	2nd storey	Beam, East of B2	All
	CR-2-C2-U	North	2nd storey	C2	All
	SR-2-C2-W	North	2nd storey	Beam, West of C2	All

Table 4. **List of strain measurements.**

Type	Nomenclature	Frame	Level	Position	Specimens
Strains	SG-0-A1-W	South	Level 0	A1, West	All
	SG-0-A1-E	South	Level 0	A1, East	All
	SG-1-A1-W	South	Level 1	A1, West	All
	SG-1-A1-E	South	Level 1	A1, East	All
	SG-2-A1-W	South	Level 2	A1, West	All, except uFrame-M
	SG-2-A1-E	South	Level 2	A1, East	All, except uFrame-M
	SG-3-A1-W	South	Level 3	A1, West	All
	SG-3-A1-E	South	Level 3	A1, East	All
	SG-0-B1-W	South	Level 0	B1, West	All
	SG-0-B1-E	South	Level 0	B1, East	All
	SG-1-B1-W	South	Level 1	B1, West	All
	SG-1-B1-E	South	Level 1	B1, East	All
	SG-2-B1-W	South	Level 2	B1, West	All, except uFrame-M
	SG-2-B1-E	South	Level 2	B1, East	All, except uFrame-M
	SG-3-B1-W	South	Level 3	B1, West	All
	SG-3-B1-E	South	Level 3	B1, East	All
	SG-0-C1-W	South	Level 0	C1, West	All
	SG-0-C1-E	South	Level 0	C1, East	All
	SG-1-C1-W	South	Level 1	C1, West	All
	SG-1-C1-E	South	Level 1	C1, East	All
	SG-2-C1-W	South	Level 2	C1, West	All, except uFrame-M
	SG-2-C1-E	South	Level 2	C1, East	All, except uFrame-M
	SG-3-C1-W	South	Level 3	C1, West	All
	SG-3-C1-E	South	Level 3	C1, East	All
	SG-0-A2-W	North	Level 0	A2, West	All
	SG-0-A2-E	North	Level 0	A2, East	All
	SG-1-A2-W	North	Level 1	A2, West	All
	SG-1-A2-E	North	Level 1	A2, East	All
	SG-2-A2-W	North	Level 2	A2, West	All
	SG-2-A2-E	North	Level 2	A2, East	All
	SG-3-A2-W	North	Level 3	A2, West	All
	SG-3-A2-E	North	Level 3	A2, East	All
	SG-0-B2-W	North	Level 0	B2, West	All
	SG-0-B2-E	North	Level 0	B2, East	All
	SG-1-B2-W	North	Level 1	B2, West	All
	SG-1-B2-E	North	Level 1	B2, East	All
	SG-2-B2-W	North	Level 2	B2, West	All
	SG-2-B2-E	North	Level 2	B2, East	All
	SG-3-B2-W	North	Level 3	B2, West	All
	SG-3-B2-E	North	Level 3	B2, East	All

Type	Nomenclature	Frame	Level	Position	Specimens
	SG-0-C2-W	North	Level 0	C2, West	All
	SG-0-C2-E	North	Level 0	C2, East	All
	SG-1-C2-W	North	Level 1	C2, West	All
	SG-1-C2-E	North	Level 1	C2, East	All
	SG-2-C2-W	North	Level 2	C2, West	All
	SG-2-C2-E	North	Level 2	C2, East	All
	SG-3-C2-W	North	Level 3	C2, West	All
	SG-3-C2-E	North	Level 3	C2, East	All
	SG-1-A1B1-S	South	1st Storey	Bracing, bottom A to top B	BFrame-M and -C
	SG-1-A1B1-N	South	1st Storey	Bracing, bottom A to top B	BFrame-M and -C
	SG-1-B1A1-S	South	1st Storey	Bracing, bottom B to top A	BFrame-M and -C
	SG-1-B1A1-N	South	1st Storey	Bracing, bottom B to top A	BFrame-M and -C
	SG-1-B1C1-S	South	1st Storey	Bracing, bottom B to top C	BFrame-M and -C
	SG-1-B1C1-N	South	1st Storey	Bracing, bottom B to top C	BFrame-M and -C
	SG-1-C1B1-S	South	1st Storey	Bracing, bottom C to top B	BFrame-M and -C
	SG-1-C1B1-N	South	1st Storey	Bracing, bottom C to top B	BFrame-M and -C
	SG-1-A2B2-S	South	2nd Storey	Bracing, bottom A to top B	BFrame-M and -C
	SG-1-A2B2-N	South	2nd Storey	Bracing, bottom A to top B	BFrame-M and -C
	SG-1-B2A2-S	South	2nd Storey	Bracing, bottom B to top A	BFrame-M and -C
	SG-1-B2A2-N	South	2nd Storey	Bracing, bottom B to top A	BFrame-M and -C
	SG-1-B2C2-S	South	2nd Storey	Bracing, bottom B to top C	BFrame-M and -C
	SG-1-B2C2-N	South	2nd Storey	Bracing, bottom B to top C	BFrame-M and -C
	SG-1-C2B2-S	South	2nd Storey	Bracing, bottom C to top B	BFrame-M and -C
	SG-1-C2B2-N	South	2nd Storey	Bracing, bottom C to top B	BFrame-M and -C
	SG-2-A1B1-S	North	1st Storey	Bracing, bottom A to top B	BFrame-M and -C
	SG-2-A1B1-N	North	1st Storey	Bracing, bottom A to top B	BFrame-M and -C
	SG-2-B1A1-S	North	1st Storey	Bracing, bottom B to top A	BFrame-M and -C
	SG-2-B1A1-N	North	1st Storey	Bracing, bottom B to top A	BFrame-M and -C
	SG-2-B1C1-S	North	1st Storey	Bracing, bottom B to top C	BFrame-M and -C
	SG-2-B1C1-N	North	1st Storey	Bracing, bottom B to top C	BFrame-M and -C
	SG-2-C1B1-S	North	1st Storey	Bracing, bottom C to top B	BFrame-M and -C
	SG-2-C1B1-N	North	1st Storey	Bracing, bottom C to top B	BFrame-M and -C
	SG-2-A2B2-S	North	2nd Storey	Bracing, bottom A to top B	BFrame-M and -C
	SG-2-A2B2-N	North	2nd Storey	Bracing, bottom A to top B	BFrame-M and -C
	SG-2-B2A2-S	North	2nd Storey	Bracing, bottom B to top A	BFrame-M and -C
	SG-2-B2A2-N	North	2nd Storey	Bracing, bottom B to top A	BFrame-M and -C
	SG-2-B2C2-S	North	2nd Storey	Bracing, bottom B to top C	BFrame-M and -C
	SG-2-B2C2-N	North	2nd Storey	Bracing, bottom B to top C	BFrame-M and -C
	SG-2-C2B2-S	North	2nd Storey	Bracing, bottom C to top B	BFrame-M and -C
	SG-2-C2B2-N	North	2nd Storey	Bracing, Bottom C to top B	BFrame-M and -C

Table 5. List and description of the tests performed.

Experiment Tag	Description	Maximum amplitude	Specimen	Purpose	Notes
b02	Dynamic Snap Back	F1 ~ 2 kN	uFrameM	Dynamic Identification	Pulling force at F1
b03	Dynamic Snap Back	F1 ~ 2 kN	uFrameM	Dynamic Identification	Pulling force at F1
c01	Monotonic Test (slab control)	120 mm	uFrameM	Quasi-static sway test	Displacement control using instruments on slabs
c02	Monotonic Test (frame control)	19 mm	uFrameM	Quasi-static sway test	Displacement control using instruments on frames
d01	Dynamic Snap Back	F1 ~ 2 kN	uFrameM	Dynamic Identification	Pulling force at F1
d02	Dynamic Snap Back	F1 ~ 2 kN	uFrameM	Dynamic Identification	Pulling force at F1
g01	Dynamic Snap Back	F1 ~ 2 kN	uFrameC	Dynamic Identification	Pulling force at F1. - D01: instrument HC3 not working properly; - D02: instrument HC3 not working properly; - D03: instrument HC3 replaced and working fine
l01	Cyclic Test (frame control)	120mm	uFrameC	Quasi-static sway test	Displacement control using instruments on frames
m02	Dynamic Snap Back		uFrameC	Dynamic Identification	Pulling force at F1
r02	Dynamic Snap Back	F1 ~ 2 kN	bFrameM	Dynamic Identification	Pulling force at F1
r11	Monotonic Test (frame control)	small cyclic tests (@1mm and 5mm) then push-over	bFrameM	Quasi-static sway test	Displacement control using instruments on frames. - D01 - cyclic and beginning of pushing - D02 - push-over test from initial “zero” position
r13	Dynamic Snap Back	F1 ~ 2 kN	bFrameM	Dynamic Identification	Pulling force at F1. - D01: 1st execution; - D02: 2nd execution. D01 and D02 are equivalent
s02	Dynamic Snap Back	F1 ~ 2 kN	bFrameC	Dynamic Identification	Pulling force at F1. - D01: sliding then fuse rupture at quite low force; - D02: sliding then fuse rupture, low force; - D03: fuse rupture, check data; - D04: fuse rupture, as wanted; - D05: fuse rupture, neglect the last part of the acquisition
t01	Cyclic Test (frame control)	135 mm	bFrameC	Quasi-static sway test	Displacement control using instruments on frames. - D01: pre-test at 1.694mm@Floor2; - D02: most of the test, then pause; - D03: acquisition with no movement; - D04: specimen brought back to initial position, then test at last amplitude.
u02	Dynamic Snap Back	F1 ~ 2 kN	bFrameC	Dynamic Identification	Pulling force at F1. -D01: empty; -D02: test data

3 mm/min, with reference to the top storey lateral displacements, for the uFrame-M and BFrame-M, respectively. Following the results of preliminary numerical models, in the unbraced frames (uFrame-M and uFrame-C), the displacement applied in the 1st storey was 54.5% of that applied in the top storey, simulating the displacement profile of the 1st longitudinal translation vibration mode. Similarly, for the braced frames (BFrame-M and BFrame-C) a ratio of 59.0% was used.

The cyclic tests were conducted at a rate of ~18 mm/min, with respect to the top storey lateral displacement. Table 6 presents the displacement histories imposed to specimens uFrame-C and BFrame-C, and Figure 37 illustrates the evolution of the inter-storey drift with the cycles. The displacement protocol included 2 cycles for each applied displacement amplitude. The first 2 increments corresponded to a 0.25% drift of the bottom (governing) storey, while 0.50% increments were applied for the remaining cycles.

Table 6. Displacement histories used in cyclic tests.

Cycle	uFrame-C					BFrame-C				
	1st Storey		2nd Storey		Time (s)	1st Storey		2nd Storey		Time (s)
	Drift	Disp. (mm)	Drift	Disp. (mm)		Drift	Disp. (mm)	Drift	Disp. (mm)	
0	0.00%	0.00	0.00%	0.00	0	0.00%	0.00	0.00%	0.00	0
1	0.25%	8.00	0.21%	14.67	47	0.25%	8.00	0.17%	13.55	44
1	-0.25%	-8.00	-0.21%	-14.67	142	-0.25%	-8.00	-0.17%	-13.55	131
1	0.00%	0.00	0.00%	0.00	189	0.00%	0.00	0.00%	0.00	174
2	0.25%	8.00	0.21%	14.67	236	0.25%	8.00	0.17%	13.55	218
2	-0.25%	-8.00	-0.21%	-14.67	330	-0.25%	-8.00	-0.17%	-13.55	305
2	0.00%	0.00	0.00%	0.00	377	0.00%	0.00	0.00%	0.00	349
3	0.50%	16.00	0.42%	29.34	472	0.50%	16.00	0.35%	27.11	436
3	-0.50%	-16.00	-0.42%	-29.34	660	-0.50%	-16.00	-0.35%	-27.11	610
3	0.00%	0.00	0.00%	0.00	755	0.00%	0.00	0.00%	0.00	697
4	0.50%	16.00	0.42%	29.34	849	0.50%	16.00	0.35%	27.11	784
4	-0.50%	-16.00	-0.42%	-29.34	1038	-0.50%	-16.00	-0.35%	-27.11	959
4	0.00%	0.00	0.00%	0.00	1132	0.00%	0.00	0.00%	0.00	1046
5	1.00%	32.00	0.83%	58.68	1321	1.00%	32.00	0.69%	54.21	1220
5	-1.00%	-32.00	-0.83%	-58.68	1698	-1.00%	-32.00	-0.69%	-54.21	1569
5	0.00%	0.00	0.00%	0.00	1887	0.00%	0.00	0.00%	0.00	1743
6	1.00%	32.00	0.83%	58.68	2076	1.00%	32.00	0.69%	54.21	1918
6	-1.00%	-32.00	-0.83%	-58.68	2453	-1.00%	-32.00	-0.69%	-54.21	2266
6	0.00%	0.00	0.00%	0.00	2642	0.00%	0.00	0.00%	0.00	2441
7	1.50%	48.00	1.25%	88.03	2925	1.50%	48.00	1.04%	81.32	2702
7	-1.50%	-48.00	-1.25%	-88.03	3491	-1.50%	-48.00	-1.04%	-81.32	3225
7	0.00%	0.00	0.00%	0.00	3774	0.00%	0.00	0.00%	0.00	3486
8	1.50%	48.00	1.25%	88.03	4057	1.50%	48.00	1.04%	81.32	3748
8	-1.50%	-48.00	-1.25%	-88.03	4623	-1.50%	-48.00	-1.04%	-81.32	4271
8	0.00%	0.00	0.00%	0.00	4906	0.00%	0.00	0.00%	0.00	4532
9	2.00%	64.00	1.67%	117.37	5283	2.00%	64.00	1.39%	108.43	4881
9	-2.00%	-64.00	-1.67%	-117.37	6038	-2.00%	-64.00	-1.39%	-108.43	5578

Cycle	uFrame-C					BFrame-C				
	1st Storey		2nd Storey		Time (s)	1st Storey		2nd Storey		Time (s)
	Drift	Disp. (mm)	Drift	Disp. (mm)		Drift	Disp. (mm)	Drift	Disp. (mm)	
9	0.00%	0.00	0.00%	0.00	6416	0.00%	0.00	0.00%	0.00	5927
10	2.00%	64.00	1.67%	117.37	6793	2.00%	64.00	1.39%	108.43	6276
10	-2.00%	-64.00	-1.67%	-117.37	7548	-2.00%	-64.00	-1.39%	-108.43	6973
10	0.00%	0.00	0.00%	0.00	7925	0.00%	0.00	0.00%	0.00	7322
11	2.50%	80.00	2.08%	146.71	8397	2.50%	80.00	1.74%	135.54	7757
11	-2.50%	-80.00	-2.08%	-146.71	9340	-2.50%	-80.00	-1.74%	-135.54	8629
11	0.00%	0.00	0.00%	0.00	9812	0.00%	0.00	0.00%	0.00	9065
12	2.50%	80.00	2.08%	146.71	10284	2.50%	80.00	1.74%	135.54	9501
12	-2.50%	-80.00	-2.08%	-146.71	11227	-2.50%	-80.00	-1.74%	-135.54	10372
12	0.00%	0.00	0.00%	0.00	11699	0.00%	0.00	0.00%	0.00	10808

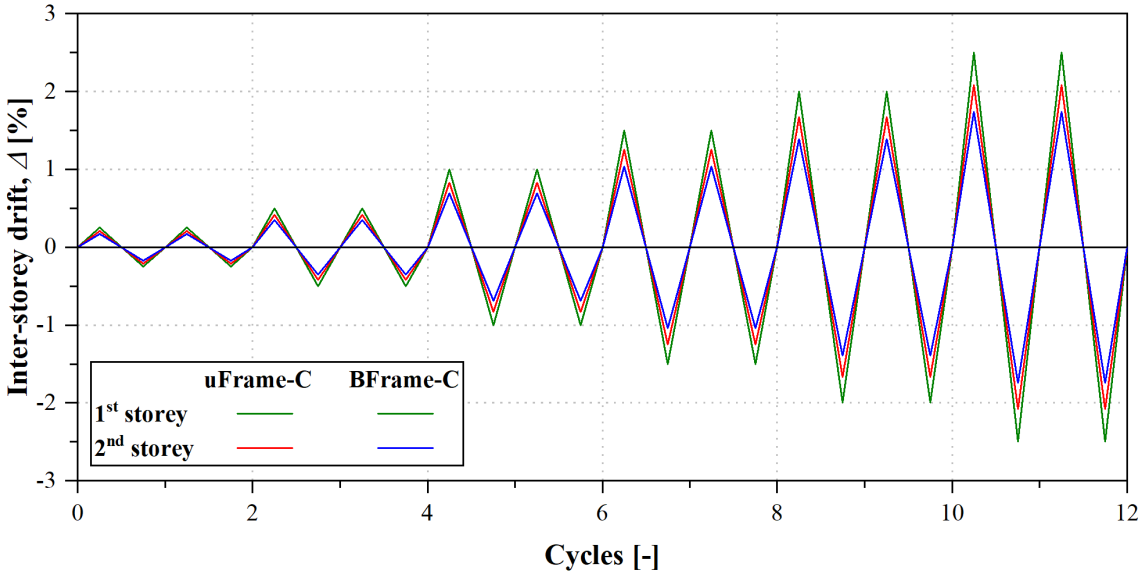

Figure 37. Displacement histories of the cyclic tests: inter-storey drift evolution.

In the first test, on specimen uFrame-M, the feedback displacements used by the control system were those measured at the slabs on the East side of the specimens (HS1 to HS4, *cf.* Figure 34 and Table 3). Following the shear connection failure on that specimen, due to the construction procedure described above (*cf.* Section Construction Phases), this led to uneven displacements of the North and South GFRP frames. Beside changing the assembling procedure, in order to avoid similar possible issues, the displacements of the remaining specimens were controlled using the quantities measured by the instruments attached to the columns on the East side of specimens (HC1 to HC4, *cf.* Figure 34 and Table 3). In any case, it should be mentioned that, except for uFrame-M, the relative displacements between the slabs and the beams were negligible.

During the tests special care was taken to avoid the global collapse of the specimens which, due to their dimensions, could endanger the personnel and damage the test equipment. In that context, the BFrame tests were stopped after extensive local damage at the bracing connections, while the uFrame tests, for which there was no apparent signs of damage, were tested up to a 2% drift at the 1st storey.

Test observations

The present section includes a very brief description of the behaviour of the specimens, as observed in the experimental tests, to supplement this data paper. A comprehensive analysis and discussion of the results will be presented in future papers.

uFrame-M

As mentioned, due to the different sequence of operations performed when assembling this first specimen, the shear connection between the concrete slab and the longitudinal beams of specimen uFrame-M was locally damaged before the test, which influenced its effectiveness. This was particularly relevant in the top North beam, as depicted in Figure 38. This damage was not noticed before the execution of the test, and resulted in an unexpected behaviour during the sway test of this specific specimen. Figure 39 shows the load *vs.* inter-storey drift curves obtained in that test. Each inter-storey drift was calculated based on the relative displacements measured at the composite columns on the East side of the specimens (*cf.* Section Set-up and instrumentation) because, although in this particular specimen the control displacements were measured at the slab, there was sliding at the damaged shear connection.

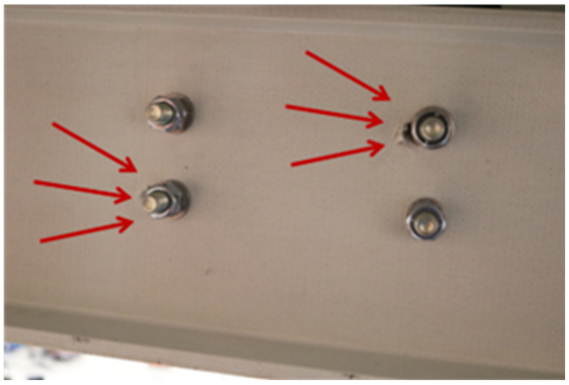

Figure 38. uFrame-M: damage at shear connection (post-test inspection).

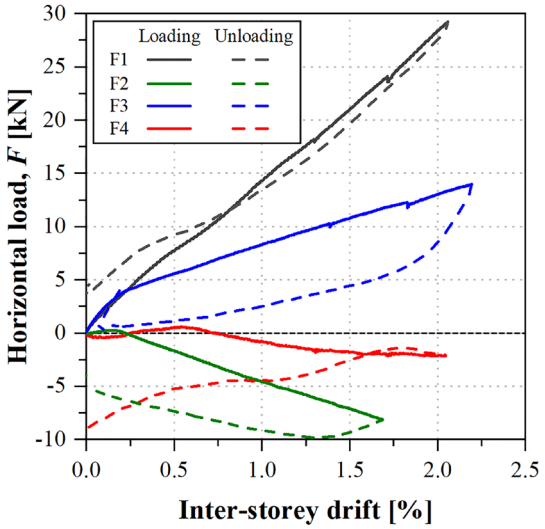

Figure 39. uFrame-M: load *vs.* inter-storey drift curves.

The results show that, in order to apply the horizontal displacements, inverse loads needed to be applied: for the 1st storey South lateral frame (F1) and 2nd storey North frame (F3), the loads were applied in the direction of the displacements, as expected, while the other actuators (F2 and F4) applied the loads in the opposite direction. Moreover, the unloading paths diverged from the loading ones, except for actuator F1. The unexpected behaviour could only be attributed to the faulty shear connection, as no other signs of damage were detected in the structure, including during the post-test inspection.

In any case, it should be highlighted that the GFRP frame endured inter-storey drifts up to 2% with no apparent signs of damage. Furthermore, the results of the snap-back tests made before and after the sway tests yielded the same mode frequencies, showing that: (i) the structure was not damaged during the test, maintaining its original stiffness; and (ii) the damage at the shear connection occurred prior to the sway test (during construction) and/or it was affecting the behaviour only in case of high lateral loads.

uFrame-C

Unlike what occurred for the uFrame-M specimen, the construction of the uFrame-C specimen followed the optimal construction protocol. In addition, and considering the issues found in the shear connection system between the longitudinal beams and the concrete floors in the previous experiment, additional steel plates were provided, strengthening the shear connection at the web of the beams. This ensured that there was no slip between the slabs and the frames; and, in fact, no signs of damage at the shear connection were registered during the test or in the post-test inspection.

Additionally, it is worth reminding that for this test (as well as for those on the braced frames), the control system was using the frame displacements measured at the East columns and not the slab displacements (initially preferred because those measurements were aligned with the loading).

During the sway test, both lateral frames presented almost symmetric behaviour for positive and negative cycles, and for both lateral frames (North and South). The load *vs.* inter-storey drift curves, depicted in Figure 40, present a quasi-bi-linear behaviour: up to ~0.3% inter-storey drifts, load increased linearly with similar stiffness for the 1st and 2nd storeys. After that point, the 1st storey loads (F1 and F4) continued to increase with the inter-storey drift but presented lower stiffness. On the other hand, the loads at the 2nd storey started to decrease. This behaviour was observed throughout the test, for every cycle, resulting in relatively wide hysteretic curves for the 2nd storey loads (F2 and F3), promoting energy dissipation.

During the tests, no signs of damage were observed, although cracking sounds were heard at the 1st cycle of 1% inter-storey drift and at the 2nd cycle of 1.5% drift (at the 1st storey).

Moreover, unlike what occurred in the previous specimen, there were slight period elongations, up to ~4%, when comparing the post-test and pre-test modal identifications, likely resulting from the ovalization of bolt holes in some connections. In any case, it should be stressed that these may only cause a minor loss of stiffness, and that the integrity of the structure was sound even after being subjected to cycling loading with -2%/+2% drifts.

BFrame-M

The braced frame presented, approximately, tri-linear behaviour, as shown in Figure 41. An initial stiffer stage, attributed to the friction of the bolted connections, was observed until ~0.04% inter-storey drifts were reached. After that stage, load increased quasi-linearly up to inter-storey drifts of ~0.18%. At this stage, crack sounds were heard, corresponding to the initiation of bearing failure at the bracing-to-column connections on the bottom floor. As the bearing failure progressed, loads continued to increase, with significantly lower stiffness and minute load drops until all 1st storey bearing connections failed (Figure 42) at ~0.75% inter-storey drifts. After that, a third stage ensued, with significantly reduced stiffness on the 1st storey - F1 and F4 (*i.e.*, the actuators loading the first floor) presented an almost horizontal plateau, while the 2nd storey stiffness remained approximately constant until the onset of bearing failure at its bearing connections (~1% inter-storey drift). Minute load drops were observed, as the bearing failure progressed and occurred on the different bracings, until all connections failed (ultimately, due to shear out), marking the end of the tests.

During the tests, the damages observed were limited to the bracing connections. The modal identification tests performed before and after the sway tests showed significant period elongation, as expected: before the sway tests, the bracings contribute to a significant increase of stiffness, while, after the sway test, the modal behaviour is similar to that of the unbraced structure, showing that the contribution of the damaged braces is negligible.

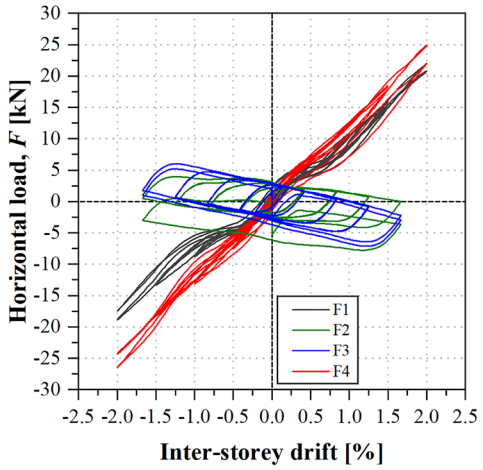

Figure 40. uFrame-C: load *vs.* inter-storey drift curves.

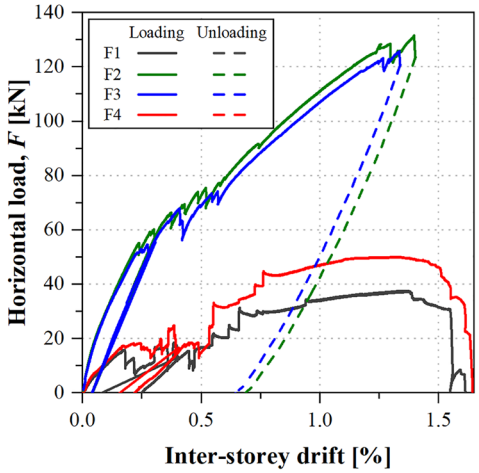

Figure 41. BFrame-M: load *vs.* inter-storey drift curves.

BFrame-C

The final specimen, a braced frame, was subjected to a cyclic test. Figure 43 shows the load *vs.* inter-storey drift curves, which are symmetric, both regarding the direction of the load and the lateral frames (South or North). The cyclic back-bone curves are similar to their monotonic counterparts (*cf.* Figure 41), although the failure of the bracing connections occurred for slightly higher inter-storey drifts. It should be stressed that, due to buckling phenomena, depicted in Figure 44, the bracings contributed to the resistance of the frame only when loaded in tension. On the other hand, the results show that such buckling phenomena did not decrease their stiffness and strength, although significant permanent deformations were observed, mainly due to plastic deformations of the gusset plates. Nevertheless, upon load reversal, the significant out-of-plane displacements of the compressed bracings (*cf.* Figure 44), stemming from flexural-torsional buckling phenomena, had to be inversed before those bracings could be

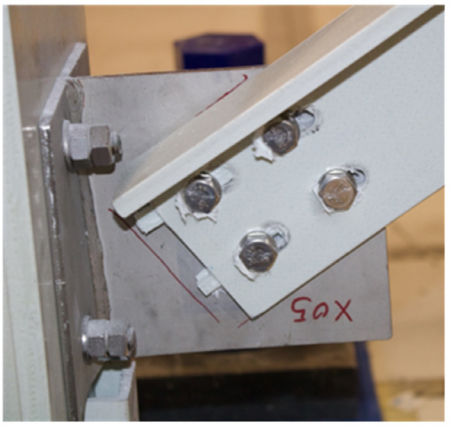

Figure 42. BFrame-M: failed bracing connection.

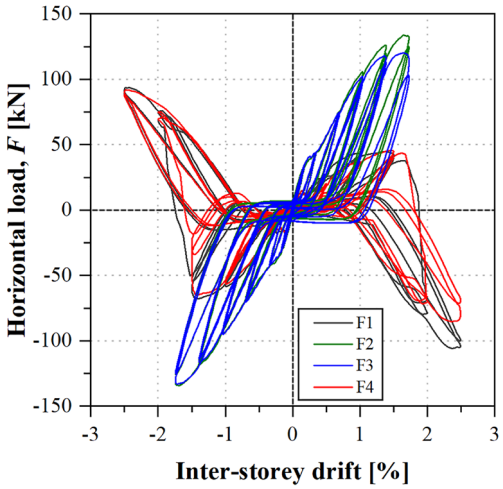

Figure 43. BFrame-C: load *vs*. inter-storey drift curves.



Figure 44. BFrame-C: significant buckling deformations of the compressed bracings.

subjected to tensile stresses, resulting in significant pinching (*cf*. Figure 43).

As for the previous braced frame, visible signs of damage were limited to the bracing connections (*cf*. Figure 42). Also, the modal identification tests yielded similar results, with significant period elongation after the sway tests, with the damaged structural response being analogous to that of the unbraced frames.

Conclusions

This paper presented the data set of the sway tests performed on full-scale GFRP frame structures at the ELSA Reaction Wall of the Joint Research Centre physical research infrastructure of the European Commission. Comprehensive details were provided on the geometry and composition of the specimens, their construction procedure, measurement equipment, test setup and test procedures. This guarantees that the data set can be understood and used by third parties.

Future publications by the authors will focus on the detailed analysis and discussion of the results, including their relevance for the drafting of seismic design guidelines, compatible with the provisions of the future Eurocode for composite structures[10].

Ethics and consent

Ethical approval and consent were not required.

Data availability

The paper briefly presents the Dissipate and Recentre (D&R) project, including all relevant information regarding the specimens, measuring equipment, test setup and test procedure. Future publications will include detailed analyses and discussion of the results. The dataset, gathering quantitative information and metadata, is made available by the authors in line with the requirement of the framework of the Open Access to JRC Research Infrastructures. The complete dataset can be downloaded at https://doi.org/10.5281/zenodo.15211782[21] under a CC BY 4.0 license.

In order to understand the structure of the shared dataset, the reader should refer to the Technical Report No JRC141264[19].

It is worth mentioning a short list of the main contents. These include (i) details of the specimens, (ii) applied loading patterns, (iii) details and calibration reports relative to the installed instrumentations (for further details on the calibration procedure refer to the Technical Report No JRC139347[22]). Besides, for each test, the dataset includes: (i) raw data as recorded by the acquisition system of the ELSA lab, (ii) processed data for an easier access to the output of the monitoring, (iii) graphical representation of the main response quantities, (iv) photo sequences taken during the execution of the testing protocol.

Acknowledgements

The authors acknowledge the contributions of all team members of the Dissipate&Recentre project who are not authors of this particular paper. The authors are also thankful for all the help and support of the staff at the JRC ELSA facility, without whom this experimental campaign could not have been successfully completed. A special thanks is due to Bruno Pereira for his continuate support and willingness to accommodate the authors' request to install additional instrumentation, and to find solutions for unforeseen difficulties.

References

1. Bank LC: **Progressive failure and ductility of FRP composites for construction: review.** *J Compos Constr.* 2013; **17**(3): 406–19.
Publisher Full Text
2. Martins D, Proença M, Correia JR, *et al.*: **Development of a novel beam-to-column connection system for pultruded GFRP tubular profiles.** *Compos Struct.* 2017; **171**: 263–276.
Publisher Full Text
3. Martins D, Proença M, Gonilha JA, *et al.*: **Experimental and numerical analysis of GFRP frame structures. Part 1: cyclic behaviour at the connection level.** *Compos Struct.* 2019a; **220**: 304–317.
Publisher Full Text
4. Martins D, Gonilha J, Correia JR, *et al.*: **Exterior beam-to-column bolted connections between GFRP I-shaped pultruded profiles using stainless steel cleats. Part 1: experimental study.** *Thin-Walled Struct.* 2021; **163**: 107719.
Publisher Full Text
5. Martins D, Gonilha J, Correia JR, *et al.*: **Monotonic and cyclic behaviour of cuff beam-to-column connection system for tubular pultruded GFRP profiles.** *Eng Struct.* 2021; **247**: 113165.
Publisher Full Text
6. Martins D, Gonilha J, Correia JR, *et al.*: **Monotonic and cyclic behaviour of a stainless steel cuff system for beam-to-column connections between pultruded I-section GFRP profiles.** *Eng Struct.* 2021; **249**: 113294.
Publisher Full Text
7. Martins D, Sá MF, Gonilha JA, *et al.*: **Experimental and numerical analysis of GFRP frame structures. Part 2: monotonic and cyclic sway behaviour of plane frames.** *Compos Struct.* 2019b; **220**: 194–208.
Publisher Full Text
8. Martins D, Gonilha J, Correia JR, *et al.*: **Monotonic and cyclic sway behaviour of 2-dimensional frames made of pultruded GFRP I-section profiles.** *Structures.* 2023; **55**: 2461–2477.
Publisher Full Text
9. Gonilha J, Martins D, Correia JR, *et al.*: **Seismic response of three-dimensional pultruded GFRP frames.** *J Compos Constr.* 2024; **28**(4): 04024021.
Publisher Full Text
10. European Committee for Standardization: **CEN/TS 19101:2022 – Design of fibre-polymer composite structures.** 2022.
Reference Source
11. M.M. Srl a socio unico: **Pultruded CE marked profiles profiles technical sheet.** 2024; Retrieved January 2024.
Reference Source
12. European Committee for Standardization: **EN 10088:2024 - stainless steels.** 2024.
Reference Source
13. American Society for Testing and Materials: **ASTM A240/A240M-23 - standard specification for chromium and chromium-nickel stainless steel plate, sheet, and strip for pressure vessels and for general applications.** 2023.
Reference Source
14. International Organization for Standardization: **ISO 3506:2020 - fasteners — mechanical properties of corrosion-resistant stainless steel fasteners.** 2020.
Reference Source
15. International Organization for Standardization: **ISO 898-1:2013 - fasteners — mechanical properties of fasteners made of carbon steel and alloy steel.** 2013.
Reference Source
16. European Committee for Standardization: **EN 2016:2013+A2:2021 – concrete – specification, performance, production and conformity.** 2021.
Reference Source
17. European Committee for Standardization: **EN 10080:2005 – steel for the reinforcement of concrete – Weldable reinforcing steel – general.** 2005.
Reference Source
18. TECNOGRIP Srl: **TECNOGRIP s.r.l. sistemi construttivi d'avanguardia. Cat. 11/06.** (n.d.); Retrieved December 2023.
Reference Source
19. Peloso S, Molina FJ, Lamperti Tornaghi M, *et al.*: **ELSA, structure of the experimental datasets.** Publications Office of the European Union, 2024.
http://www.doi.org/10.2760/6543699
20. Peroni M, Pegon P, Molina FJ, *et al.*: **Ethernet-based servo-hydraulic real-time controller and DAQ at ELSA for large scale experiments.** *J Earthq Eng.* 2022; **26**(15): 7657–7688.
Publisher Full Text
21. **http://www.doi.org/10.5281/zenodo.15211782**
22. European Commission, Peloso S, Molina FJ, *et al.*: **ELSA - Procedure for calibration and verification of displacement and rotation measuring systems.** Publications Office of the European Union, Luxembourg, JRC139347, 2024.
http://www.doi.org/10.2760/3562031

Open Peer Review

Current Peer Review Status: ✔ ? ✔ ✔

Version 2

Reviewer Report 11 February 2026

https://doi.org/10.21956/openreseurope.24516.r68655

© **2026 Calabrese A.** This is an open access peer review report distributed under the terms of the Creative Commons Attribution License, which permits unrestricted use, distribution, and reproduction in any medium, provided the original work is properly cited.

✔ **Angelo Savio Calabrese**
Politecnico di Milano, Milan, Italy

The repository provides a clearly curated experimental dataset that is presented with a strong emphasis on transparency, traceability, and practical reusability. The documentation of the testing campaign, including data organization, metadata, and supporting files, allows the reader to readily understand how the data were generated and how they can be accessed and reused without ambiguity. The authors demonstrate good practice in openly reporting experimental choices, test conditions, and deviations encountered during the campaign, which enhances the credibility of the dataset and supports reproducibility. Overall, the work appears robust and well prepared for reuse by both academic and applied researchers, and it represents a useful contribution within the scope and objectives of a data article.

Given the completeness and level of detail of the report, the comments below are solely intended to invite the authors to enrich the article by sharing practical recommendations derived from the experience gained during the experimental campaign. As is often the case when an experimental program is completed, hindsight may highlight aspects that could have been addressed differently or improved if the study were to be repeated. In this spirit, the following comments are intended to encourage the authors to reflect on and document this “lessons learned” perspective, based on their direct experimental experience.

1 - The authors are kindly asked to clarify the rationale adopted for the structural design of the tested frame, particularly in relation (if any) to the recently issued PD CEN/TS 19101:2022, *“Design of fibre-polymer composite structures".* It would be useful to understand whether the indications provided by this document were considered at any stage of the design process, and how applicable the authors judge such design guidance to be when confronted with the practical execution of a real, multi-storey GFRP structure. Given that this frame represents one of the few early examples of a multi-storey structure realized using structural GFRP profiles, the authors’ critical assessment of the applicability and limitations of current design recommendations would be of clear value to future designers and researchers.

2 - The discussion of the experimental results would benefit from a final section in which the

authors summarize their experience-based suggestions on how the design of similar GFRP structures could be improved and made more effective. In this respect, the structural connections appear to represent a "weak link" of the overall system performance. The authors are encouraged to discuss how connection design could be enhanced, and whether alternative solutions, such as fully bonded or hybrid bonded–bolted connections, may provide improved performance compared to the configurations tested in the present study.

3 - It would be useful to assess whether a direct correlation can be established between the pin-bearing strength of the GFRP material reported in Table 1 and the observed failure of the structural connections, particularly when connection failure governs the global crisis of the structure. Clarifying this relationship, even at a qualitative or semi-quantitative level, would improve the interpretability of the dataset and support its reuse for connection modelling and design-oriented studies.

4 - Both local and global buckling of GFRP structural elements appear to limit the exploitation of the full capacity of the tested frame. The authors are encouraged to comment on potential strategies, based on their experimental experience, to mitigate buckling phenomena in similar structures (at the design stage). Such insights would further enhance the practical value of the dataset for researchers and practitioners interested in the development of efficient and reliable GFRP framing systems.

Is the rationale for creating the dataset(s) clearly described?

Yes

Are the protocols appropriate and is the work technically sound?

Yes

Are sufficient details of methods and materials provided to allow replication by others?

Yes

Are the datasets clearly presented in a useable and accessible format?

Yes

Competing Interests: No competing interests were disclosed.

Reviewer Expertise: My research has focused in particular on the static and fatigue behavior of composite materials for structural applications, with special attention to both fully composite structures and externally bonded strengthening systems applied to existing steel, concrete, and masonry structures.

I confirm that I have read this submission and believe that I have an appropriate level of expertise to confirm that it is of an acceptable scientific standard.

Reviewer Report 10 February 2026

https://doi.org/10.21956/openreseurope.24516.r68657

© 2026 Vafaei M. This is an open access peer review report distributed under the terms of the Creative Commons Attribution License, which permits unrestricted use, distribution, and reproduction in any medium, provided the original work is properly cited.

Mohammadreza Vafaei
Universiti Teknologi Malaysia, Johor, Malaysia

The manuscript presents experimental results from four large-scale composite frame structures subjected to gravity and cyclic loading. The paper is well-written and offers valuable insights into the fabrication, testing protocols, and subsequent performance of these systems. However, additional details regarding the design methodology and specific failure modes are required to improve the clarity and reproducibility of the study. Addressing the following comments will enhance the quality of the manuscript.

Specific Comments

1. Design Methodology and Loading: The rationale behind the member sizing (beams, columns, and braces) requires further elaboration. Please include the specific design concepts and standards used. Specifically, provide the values for the design dead loads, live loads, and seismic parameters that governed the selection of these member sizes.

2. Connection Details: Please provide a more granular description of the connection design process. It would be beneficial to include design method and standard used to determine the number of bolts and bolt dimensions for both beam-to-column and brace-to-column connections.

3. Beam-to-Column Connection Behavior: The detailing employed for the beam-to-column connections suggests a semi-rigid response. Please justify the selection of this specific detail. Was this intended to model a specific existing construction practice?

4. Bearing Failure Analysis: Figures 38 and 42 appear to indicate bearing failure. Please clarify if this specific failure mode was anticipated and accounted for during the design stage (e.g., via checking bearing limit states vs. bolt shear).

5. Work-Point Eccentricity: Figure 10 shows that the brace centerline does not intersect with the column centerline (work-point eccentricity). This configuration imposes additional bending moments on the columns. Please explain the reasoning behind this detailing choice and discuss how the additional moment demands were accounted for in the column design.

6. Suitability of Single Angle Braces: Single angle braces are generally not recommended for Special Concentrically Braced Frames (SCBF) due to their susceptibility to flexural buckling and potential for poor cyclic performance. Please justify the use of single angles in this study. Furthermore, please provide the slenderness ratio.

7. Strain Data: The current manuscript lacks measured strain data. The inclusion of strain histories is beneficial to better understand the cyclic response of the frames.

Is the rationale for creating the dataset(s) clearly described?

Yes

Are the protocols appropriate and is the work technically sound?
Yes

Are sufficient details of methods and materials provided to allow replication by others?
Partly

Are the datasets clearly presented in a useable and accessible format?
Yes

Competing Interests: No competing interests were disclosed.

Reviewer Expertise: Seismic design and retrofitting, Vibration control , Structural health monitoring

I confirm that I have read this submission and believe that I have an appropriate level of expertise to confirm that it is of an acceptable scientific standard.

Reviewer Report 19 January 2026

https://doi.org/10.21956/openreseurope.24516.r68076

© 2026 Civera M. This is an open access peer review report distributed under the terms of the Creative Commons Attribution License, which permits unrestricted use, distribution, and reproduction in any medium, provided the original work is properly cited.

Marco Civera
Polytechnic of Turin, Turin, Piedmont, Italy

The revised version is fully compliant.

Competing Interests: No competing interests were disclosed.

Reviewer Expertise: Structural Health Monitoring and Damage Assessment

I confirm that I have read this submission and believe that I have an appropriate level of expertise to confirm that it is of an acceptable scientific standard.

Version 1

Reviewer Report 13 November 2025

https://doi.org/10.21956/openreseurope.22184.r62457

© 2025 Al-Thairy H. This is an open access peer review report distributed under the terms of the Creative Commons Attribution License, which permits unrestricted use, distribution, and reproduction in any medium, provided the original work is properly cited.

?

Haitham Al-Thairy
[1] University of Al-Qadisiyah, Al Diwaniyah, Al Diwaniyah, Iraq
[2] University of Al-Qadisiyah, Al Diwaniyah, Al Diwaniyah, Iraq

This article presents a data set of a full-scale experimental test of four GFRP two bay two story frames under static and quasi cyclic static load. Two of the frames are unbraced while the other two are braced against lateral movement. The frames are subjected to a displacement control loading up to global or local damage of the frames on a west side of the farms and the inert-story drift were measured at each story level at the east side of the frames. The experimental programed was described in terms of the material, geometry, test setup, loading scheme data collection and recording devices Also, a primarily data were presented in terms of the load- inert-story drift for each frame considered in the tests. The research project is very interesting in terms of qualifying the lateral resilience of GFRP frames under seismic events and the determine the potential of using advantageous properties of GFRP such as the high tensile strength, low density and low inertia force in reducing the damage of structures and saving the human lives. However, the following comments are suggested by the reviewer:

1. A pre cast concrete slab is attached to the GFRP beams to simulate the equivalent vertical loads of a real application, and allowing to anchor the actuators as suggested by the authors. On the other hand, it has been mentioned in another place of the manuscript that " It should be stressed that the concrete slabs are not part of the conceptual design of the specimens (in an actual all-composite structure, the floors would likely be made of composite sandwich panels), serving only as a mean to apply vertical (dead) and horizontal (connected to the actuator) loads without suffering any damage during the tests". However, the existence of the concrete slabs significantly affects the behavior of the frames in terms of increasing the total weight of the frame and requiring additional details such as shear connectors, bolts, etc. These effects increase the potential failure of the frames globally due to inertia effects and locally due to failure of the connection's details between the slab and the beams
2. A displacement history imposed to specimens to simulate the tests at a rate of18 mm/min. However, it is more rational to apply displacement time history which is normally much higher the rate to simulate a real earthquake displacement or acceleration.
3. Please explain why hysteretic curves the top stories (F2, F3) forces are in a reverse direction of the bottom stories (F1, F4) ?
4. Please present the symbols of the forces in a sequential order (i.e. F1, F2, ..) in the legend of the curves

Is the rationale for creating the dataset(s) clearly described?
Partly

Are the protocols appropriate and is the work technically sound?
Partly

Are sufficient details of methods and materials provided to allow replication by others?

Yes

Are the datasets clearly presented in a useable and accessible format?
Yes

Competing Interests: No competing interests were disclosed.

Reviewer Expertise: behavior and failure of GFRP RC members , dynamic analysis of structures, developing analytics methods of the static and dynamic analysis of structures particularly structures under impact and blast.

I confirm that I have read this submission and believe that I have an appropriate level of expertise to confirm that it is of an acceptable scientific standard, however I have significant reservations, as outlined above.

Author Response 02 Jan 2026

Jose Gonilha

The authors thank the reviewer for the overall positive assessment of the paper. Below, you can find a detailed reply to each of your specific comments:
Reply 1: The authors agree that the presence of the concrete slab influences the behaviour of the frame, particularly due to the increase in total weight. However, we would like to raise the attention of the reviewer to the fact that this was precisely the objective of using the concrete slabs: to simulate the weight of a floor system used in composite structures (e.g., sandwich panels), the weight of other permanent loads (partition walls, furniture, etc), and the quasi-permanent part of the live loads, thereby encompassing the weight used in the seismic design combination. Additionally, the authors acknowledge that local failure of the connection details is a possibility, which was prevented by overdesigning these connections – note that the localized failure in the shear connection that was observed (in a single specimen) was due to an error in the construction process, and did not occur during the test. Moreover, as stated in the manuscript, the “design of the slabs guaranteed that there was no concrete-GFRP composite action in the vicinity of the supports, and that the slabs did not transmit bending moments from one span to the other”; this minimizes the composite action between the beams and the slabs, localizing it at the centre of the spans, which play a smaller role in the sway behaviour of the frames.
Reply 2: The use of quasi-static experimental tests to simulate the response of structures to earthquake actions is a well-established practice (e.g., https://doi.org/10.1193/1.1585869). This technique allows the cost-effective assessment of structural systems, particularly at large scales, contributing with a wealth of data that allows to determine their seismic behaviour. It should also be noted that the data obtained with sway-tests closely relates with that of seismic design procedures, namely P-delta analysis. Furthermore, the outcomes of cyclic tests are recognised as the most suitable for the estimation of structural capacity, and the calibration of numerical models, also due to the valuable information about the stability of structural response and energy-dissipation capacity.
Reply 3: The different signs of the top and bottom storey loads are attributed to the fact that the displacement history imposed on the specimens diverged, at some point, from the

first modal configuration of the specimens. As mentioned in the paper, the modal shapes were obtained from preliminary numerical models. In practice, when the stiffness of the connections change, in this case due to surpassing the friction limit, the modal characteristics of the structure change. This can result in the imposition of an unnatural deformations, namely regarding the top/bottom displacement ratios. This discussion has not been included in this paper because this is a data paper, focused on providing all experimental data and information about the test results. Future papers will focus on the analysis and discussion of the results. It can be added that the authors know this effect could have been avoided adopting different control strategies. For instance, imposing displacement-controlled cycles at the second floor, while applying force-controlled cycles (e.g. imposing a constant ratio between the forces at the first and at the second stories equal to 0.5) would have avoided the story-forces to counteract each other. On the other hand, such a loading strategy would have activated a soft-story mechanisms preventing the possibility to achieve the maximum capacity of the second storey.
Reply 4: The plots (Figures 39, 41, 40, and 43) have been changed following the reviewer's recommendation.

Competing Interests: No competing interests were disclosed.

Reviewer Report 03 November 2025

https://doi.org/10.21956/openreseurope.22184.r62458

© **2025 Civera M.** This is an open access peer review report distributed under the terms of the Creative Commons Attribution License, which permits unrestricted use, distribution, and reproduction in any medium, provided the original work is properly cited.

Marco Civera
[1] Polytechnic of Turin, Turin, Piedmont, Italy
[2] Polytechnic of Turin, Turin, Piedmont, Italy

The repository described by this report represents a valuable dataset of full-scale GFRP frames, with rich instrumentation and clear test logs. The note is strong, and the experimental data are reusable and of interest to the scientific and technical community.

The dataset, specimens, set-up, instrumentation, and test programs are all succinctly, transparently, and efficiently described.

Most importantly, the use of full-scale models is highly relevant for accounting for potential scale effects that are generally dismissed in scaled-down laboratory replicas.

The investigated frames are realistic, also in their braced/unbraced variants and (nominal) mass distribution.

Notes on apparent damage (or lack thereof) are coherent and explicitly detailed. The bracing

connection failure taxonomy is also clear and understandable.

The hardware details are good and explicit.

Issues such as connection assembly problems are openly and honestly reported (see uFrame-M). Countermeasures adopted for other specimens are clearly detailed.

The instrumentation is particularly rich, including calibration reports.

The level of detail in the test log is also laudable.

The dataset directly enables several reuse scenarios, from Finite Element model calibration for GFRP frames (also accounting for material orthotropy and bolted joints), pinched hysteresis models for braced systems, connection fragility/limit states, and validation of control strategies.

All being said, the dataset is well-structured and a very good contribution. Especially since GFRP offers an attractive package for building frames: very high specific strength at a fraction of steel's weight (thus requiring smaller foundations and producing a lower seismic mass), competitive specific stiffness, low thermal conductivity for reduced thermal bridging, and outstanding corrosion resistance that virtually eliminates chloride- or moisture-driven deterioration.

Most importantly, Pultruded members deliver consistent, factory-controlled quality and enable rapid, lightweight construction. Well-detailed GFRP systems can provide a stable cyclic response with minimal residual deformation. Hence, in the near future, GFRP unlocks durable, low-maintenance, fast-to-install structures with compelling whole-life benefits; this report, the dataset it describes, and the funded research go in the right direction for these aims.

Is the rationale for creating the dataset(s) clearly described?
Yes

Are the protocols appropriate and is the work technically sound?
Yes

Are sufficient details of methods and materials provided to allow replication by others?
Yes

Are the datasets clearly presented in a useable and accessible format?
Yes

Competing Interests: No competing interests were disclosed.

Reviewer Expertise: Structural Health Monitoring and Damage Assessment

I confirm that I have read this submission and believe that I have an appropriate level of expertise to confirm that it is of an acceptable scientific standard.

Author Response 02 Jan 2026

Jose Gonilha

The authors greatly appreciate the comprehensive assessment of the paper made by the reviewer.

Competing Interests: No competing interests were disclosed.